EFT Validity and Unitarity for Tri/Multi-Boson Signatures

Rafael L. Delgado (work with C. García García, M.J. Herrero)

$pp \to W^+W^- j_1 j_2$

by $W^+W^- \to W^+W^-$ scattering

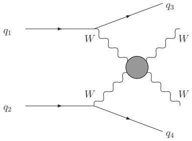

$pp \to WZ j_1 j_2$

by $WZ \to WZ$ scattering

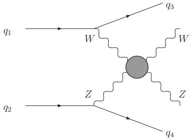

Multi-Boson Interactions 2019

Linear vs. non–linear: linear representation

- The ω^a and h fit in a left $SU(2)$ doublet.
- The Higgs always appears in the combination $h + v$.
- Typical situation when h is a fundamental field.
- Based in a **cutoff Λ expansion**: $\mathcal{O}(d)/\Lambda^{d-4}$, d and operator of dimension $d = 4, 6, 8, \ldots$.
- The usual approach, based on considering a full basis, allows to make a well-defined biyection between bases, at the price of reaching a high number of operators ($> 10^3$ for dim-8).
- EFT typically emerging from weakly interacting High Energy (HE) Theory.

Linear vs. non–linear: linear representation

- The ω^a and h fit in a left $SU(2)$ doublet.
- The Higgs always appears in the combination $h+v$.
- Typical situation when h is a fundamental field.
- Based in a **cutoff Λ expansion**: $\mathcal{O}(d)/\Lambda^{d-4}$, d and operator of dimension $d=4,6,8,\ldots.$
- The usual approach, based on considering a full basis, allows to make a well-defined biyection between bases, at the price of reaching a high number of operators ($>10^3$ for dim-8).
- EFT typically emerging from weakly interacting High Energy (HE) Theory.

Linear vs. non–linear: linear representation

- The ω^a and h fit in a left $SU(2)$ doublet.
- The Higgs always appears in the combination $h + v$.
- Typical situation when h is a fundamental field.
- Based in a **cutoff Λ expansion**: $\mathcal{O}(d)/\Lambda^{d-4}$, d and operator of dimension $d = 4, 6, 8, \ldots$.
- The usual approach, based on considering a full basis, allows to make a well-defined biyection between bases, at the price of reaching a high number of operators ($> 10^3$ for dim-8).
- EFT typically emerging from weakly interacting High Energy (HE) Theory.

Linear vs. non–linear: linear representation

- The ω^a and h fit in a left $SU(2)$ doublet.
- The Higgs always appears in the combination $h + v$.
- Typical situation when h is a fundamental field.
- Based in a **cutoff Λ expansion**: $\mathcal{O}(d)/\Lambda^{d-4}$, d and operator of dimension $d = 4, 6, 8, ...$
- The usual approach, based on considering a full basis, allows to make a well-defined biyection between bases, at the price of reaching a high number of operators ($> 10^3$ for dim-8).
- EFT typically emerging from weakly interacting High Energy (HE) Theory.

Linear vs. non–linear: linear representation

- The ω^a and h fit in a left $SU(2)$ doublet.
- The Higgs always appears in the combination $h+v$.
- Typical situation when h is a fundamental field.
- Based in a **cutoff Λ expansion**: $\mathcal{O}(d)/\Lambda^{d-4}$, d and operator of dimension $d=4,6,8,....$
- The usual approach, based on considering a full basis, allows to make a well-defined biyection between bases, at the price of reaching a high number of operators ($>10^3$ for dim-8).
- EFT typically emerging from weakly interacting High Energy (HE) Theory.

Linear vs. non–linear: linear representation

- The ω^a and h fit in a left $SU(2)$ doublet.
- The Higgs always appears in the combination $h+v$.
- Typical situation when h is a fundamental field.
- Based in a **cutoff Λ expansion**: $\mathcal{O}(d)/\Lambda^{d-4}$, d and operator of dimension $d=4,6,8,....$
- The usual approach, based on considering a full basis, allows to make a well-defined biyection between bases, at the price of reaching a high number of operators ($>10^3$ for dim-8).
- EFT typically emerging from weakly interacting High Energy (HE) Theory.

Linear vs. non–linear: **non–linear representation**

- **Our work is based on this framework.**
- h is a $SU(2)$ singlet and ω^a are coordinates on a coset:

$$SU(2)_L \times SU(2)_R/SU(2)_V = SU(2) = S^3$$

- ECLh with $F(h)$ insertions.
- **Derivative expansion** ($\leftrightarrow$ Chiral expansion)
- Some higher order operators, like a_4 and a_5, that were dim-8 in the linear representation, can contribute to a lower order in the non–linear one (dim-4 in the Chiral expansion).
- Appropriate for composite models of the SBS (h as a GB).
- EFT typically emerging from strongly interacting High Energy (HE) Theory and consistent with the presence of the GAP.

Linear vs. non–linear: **non–linear representation**

- **Our work is based on this framework.**
- h is a $SU(2)$ singlet and ω^a are coordinates on a coset:

$$SU(2)_L \times SU(2)_R / SU(2)_V = SU(2) = S^3$$

- ECLh with $F(h)$ insertions.
- **Derivative expansion** ($\leftrightarrow$ Chiral expansion)
- Some higher order operators, like a_4 and a_5, that were dim-8 in the linear representation, can contribute to a lower order in the non–linear one (dim-4 in the Chiral expansion).
- Appropriate for composite models of the SBS (h as a GB).
- EFT typically emerging from strongly interacting High Energy (HE) Theory and consistent with the presence of the GAP.

Linear vs. non–linear: **non–linear representation**

- **Our work is based on this framework.**
- h is a $SU(2)$ singlet and ω^a are coordinates on a coset:

$$SU(2)_L \times SU(2)_R / SU(2)_V = SU(2) = S^3$$

- ECLh with $F(h)$ insertions.
- **Derivative expansion** ($\leftrightarrow$ Chiral expansion)
- Some higher order operators, like a_4 and a_5, that were dim-8 in the linear representation, can contribute to a lower order in the non–linear one (dim-4 in the Chiral expansion).
- Appropriate for composite models of the SBS (h as a GB).
- EFT typically emerging from strongly interacting High Energy (HE) Theory and consistent with the presence of the GAP.

Linear vs. non–linear: **non–linear representation**

- **Our work is based on this framework.**
- h is a $SU(2)$ singlet and ω^a are coordinates on a coset:

$$SU(2)_L \times SU(2)_R / SU(2)_V = SU(2) = S^3$$

- ECLh with $F(h)$ insertions.
- **Derivative expansion** (↔ Chiral expansion)
- Some higher order operators, like a_4 and a_5, that were dim-8 in the linear representation, can contribute to a lower order in the non–linear one (dim-4 in the Chiral expansion).
- Appropriate for composite models of the SBS (h as a GB).
- EFT typically emerging from strongly interacting High Energy (HE) Theory and consistent with the presence of the GAP.

Linear vs. non–linear: **non–linear representation**

- **Our work is based on this framework.**
- h is a $SU(2)$ singlet and ω^a are coordinates on a coset:

$$SU(2)_L \times SU(2)_R/SU(2)_V = SU(2) = S^3$$

- ECLh with $F(h)$ insertions.
- **Derivative expansion** (↔ Chiral expansion)
- Some higher order operators, like a_4 and a_5, that were dim-8 in the linear representation, can contribute to a lower order in the non–linear one (dim-4 in the Chiral expansion).
- Appropriate for composite models of the SBS (h as a GB).
- EFT typically emerging from strongly interacting High Energy (HE) Theory and consistent with the presence of the GAP.

Linear vs. non–linear: **non–linear representation**

- **Our work is based on this framework.**
- h is a $SU(2)$ singlet and ω^a are coordinates on a coset:

$$SU(2)_L \times SU(2)_R / SU(2)_V = SU(2) = S^3$$

- ECLh with $F(h)$ insertions.
- **Derivative expansion** (↔ Chiral expansion)
- Some higher order operators, like a_4 and a_5, that were dim-8 in the linear representation, can contribute to a lower order in the non–linear one (dim-4 in the Chiral expansion).
- Appropriate for composite models of the SBS (h as a GB).
- EFT typically emerging from strongly interacting High Energy (HE) Theory and consistent with the presence of the GAP.

Linear vs. non–linear: **non–linear representation**

- **Our work is based on this framework.**
- h is a $SU(2)$ singlet and ω^a are coordinates on a coset:

$$SU(2)_L \times SU(2)_R/SU(2)_V = SU(2) = S^3$$

- ECLh with $F(h)$ insertions.
- **Derivative expansion** ($\leftrightarrow$ Chiral expansion)
- Some higher order operators, like a_4 and a_5, that were dim-8 in the linear representation, can contribute to a lower order in the non–linear one (dim-4 in the Chiral expansion).
- Appropriate for composite models of the SBS (h as a GB).
- EFT typically emerging from strongly interacting High Energy (HE) Theory and consistent with the presence of the GAP.

Other Monte-Carlo generators with unitarity or form-factors

- **Whizard, model SM_km**. Orign. based on [A.Alboteanu,W.Kilian,J.Reuter, JHEP**0811** (2008) 010].
- Caveat: usage of the K-matrix method. Now, upgraded to T-matrix.
- Basically, a form-factor to avoid breaking unitarity bound. Not based on analytical continuation.
- Goal: estimation of unitarity constraints over perturbative regime.
- Goal: inclusion of BSM resonances on *SM_km* as effective vertices.
- **SHERPA**, Form Factor approach.

Other Monte-Carlo generators with unitarity or form-factors

- **Whizard, model SM_km**. Orign. based on [A.Alboteanu,W.Kilian,J.Reuter, JHEP**0811** (2008) 010].
- Caveat: usage of the K-matrix method. Now, upgraded to T-matrix.
- Basically, a form-factor to avoid breaking unitarity bound. Not based on analytical continuation.
- Goal: estimation of unitarity constraints over perturbative regime.
- Goal: inclusion of BSM resonances on *SM_km* as effective vertices.
- **SHERPA**, Form Factor approach.

Other Monte-Carlo generators with unitarity or form-factors

- **Whizard, model SM_km**. Orign. based on [A.Alboteanu,W.Kilian,J.Reuter, JHEP**0811** (2008) 010].
- Caveat: usage of the K-matrix method. Now, upgraded to T-matrix.
- Basically, a form-factor to avoid breaking unitarity bound. Not based on analytical continuation.
- Goal: estimation of unitarity constraints over perturbative regime.
- Goal: inclusion of BSM resonances on *SM_km* as effective vertices.
- **SHERPA**, Form Factor approach.

Other Monte-Carlo generators with unitarity or form-factors

- **Whizard, model SM_km**. Orign. based on [A.Alboteanu,W.Kilian,J.Reuter, JHEP**0811** (2008) 010].
- Caveat: usage of the K-matrix method. Now, upgraded to T-matrix.
- Basically, a form-factor to avoid breaking unitarity bound. Not based on analytical continuation.
- Goal: estimation of unitarity constraints over perturbative regime.
- Goal: inclusion of BSM resonances on *SM_km* as effective vertices.
- **SHERPA**, Form Factor approach.

Other Monte-Carlo generators with unitarity or form-factors

- **Whizard, model SM_km**. Orign. based on [A.Alboteanu,W.Kilian,J.Reuter, JHEP**0811** (2008) 010].
- Caveat: usage of the K-matrix method. Now, upgraded to T-matrix.
- Basically, a form-factor to avoid breaking unitarity bound. Not based on analytical continuation.
- Goal: estimation of unitarity constraints over perturbative regime.
- Goal: inclusion of BSM resonances on *SM_km* as effective vertices.
- **SHERPA**, Form Factor approach.

Other Monte-Carlo generators with unitarity or form-factors

- **Whizard, model SM_km**. Orign. based on [A.Alboteanu,W.Kilian,J.Reuter, JHEP**0811** (2008) 010].
- Caveat: usage of the K-matrix method. Now, upgraded to T-matrix.
- Basically, a form-factor to avoid breaking unitarity bound. Not based on analytical continuation.
- Goal: estimation of unitarity constraints over perturbative regime.
- Goal: inclusion of BSM resonances on *SM_km* as effective vertices.
- **SHERPA**, Form Factor approach.

Our approach

- We have theoretical background on comparing different unitarization procedures, and on their motivation: [Phys.Rev.Lett.**114**, 221803], [PRD**91**, 075017], [JHEP**140**, 149],...
- However, we were lacking an independent Monte Carlo implementation of the unitarized models.
- We are filling this gap [Work in progr.], [JHEP**1811** 010], [JHEP**1811**, 010], [JHEP**1711**, 098], [Eur.Phys.J.C**77** no.7, 436], [Eur.Phys.J.C**77** no.4].
    - (Weak) couplings with other initial or final states: $\gamma\gamma$, $t\bar{t}$.
    - Developing a UFO model for MadGraph v5.
- We choose MadGraph v5 because of its *easy* interfacing with other programs in the Monte Carlo chain. Both from the analytical side (FeynRules) and on the computational one (lhapdf6, Pythia, DELPHES, ExRootAnalysis, MadAnalysis 5,...).
- But we acknowledge the big improvements of other options (like Whizard and SHERPA) on this topic.

Our approach

- We have theoretical background on comparing different unitarization procedures, and on their motivation: [Phys.Rev.Lett.**114**, 221803], [PRD**91**, 075017], [JHEP**140**, 149],...
- However, we were lacking an independent Monte Carlo implementation of the unitarized models.
- We are filling this gap [Work in progr.], [JHEP**1811** 010], [JHEP**1811**, 010], [JHEP**1711**, 098], [Eur.Phys.J.C**77** no.7, 436], [Eur.Phys.J.C**77** no.4].
  - (Weak) couplings with other initial or final states: $\gamma\gamma$, $t\bar{t}$.
  - Developing a UFO model for MadGraph v5.
- We choose MadGraph v5 because of its *easy* interfacing with other programs in the Monte Carlo chain. Both from the analytical side (FeynRules) and on the computational one (lhapdf6, Pythia, DELPHES, ExRootAnalysis, MadAnalysis 5,...).
- But we acknowledge the big improvements of other options (like Whizard and SHERPA) on this topic.

Our approach

- We have theoretical background on comparing different unitarization procedures, and on their motivation: [Phys.Rev.Lett.**114**, 221803], [PRD**91**, 075017], [JHEP**140**, 149],...
- However, we were lacking an independent Monte Carlo implementation of the unitarized models.
- We are filling this gap [Work in progr.], [JHEP**1811** 010], [JHEP**1811**, 010], [JHEP**1711**, 098], [Eur.Phys.J.C**77** no.7, 436], [Eur.Phys.J.C**77** no.4].
  - (Weak) couplings with other initial or final states: $\gamma\gamma$, $t\bar{t}$.
  - Developing a UFO model for MadGraph v5.
- We choose MadGraph v5 because of its *easy* interfacing with other programs in the Monte Carlo chain. Both from the analytical side (FeynRules) and on the computational one (lhapdf6, Pythia, DELPHES, ExRootAnalysis, MadAnalysis 5,...).
- But we acknowledge the big improvements of other options (like Whizard and SHERPA) on this topic.

Our approach

- We have theoretical background on comparing different unitarization procedures, and on their motivation: [Phys.Rev.Lett.**114**, 221803], [PRD**91**, 075017], [JHEP**140**, 149],...
- However, we were lacking an independent Monte Carlo implementation of the unitarized models.
- We are filling this gap [Work in progr.], [JHEP**1811** 010], [JHEP**1811**, 010], [JHEP**1711**, 098], [Eur.Phys.J.C**77** no.7, 436], [Eur.Phys.J.C**77** no.4].
  - (Weak) couplings with other initial or final states: $\gamma\gamma$, $t\bar{t}$.
  - Developing a UFO model for MadGraph v5.
- We choose MadGraph v5 because of its *easy* interfacing with other programs in the Monte Carlo chain. Both from the analytical side (FeynRules) and on the computational one (lhapdf6, Pythia, DELPHES, ExRootAnalysis, MadAnalysis 5,...).
- But we acknowledge the big improvements of other options (like Whizard and SHERPA) on this topic.

Our approach

- We have theoretical background on comparing different unitarization procedures, and on their motivation: [Phys.Rev.Lett.**114**, 221803], [PRD**91**, 075017], [JHEP**140**, 149],...
- However, we were lacking an independent Monte Carlo implementation of the unitarized models.
- We are filling this gap [Work in progr.], [JHEP**1811** 010], [JHEP**1811**, 010], [JHEP**1711**, 098], [Eur.Phys.J.C**77** no.7, 436], [Eur.Phys.J.C**77** no.4].
    - (Weak) couplings with other initial or final states: $\gamma\gamma$, $t\bar{t}$.
    - Developing a UFO model for MadGraph v5.
- We choose MadGraph v5 because of its *easy* interfacing with other programs in the Monte Carlo chain. Both from the analytical side (FeynRules) and on the computational one (lhapdf6, Pythia, DELPHES, ExRootAnalysis, MadAnalysis 5,...).
- But we acknowledge the big improvements of other options (like Whizard and SHERPA) on this topic.

Our approach

- We have theoretical background on comparing different unitarization procedures, and on their motivation: [Phys.Rev.Lett.**114**, 221803], [PRD**91**, 075017], [JHEP**140**, 149],...
- However, we were lacking an independent Monte Carlo implementation of the unitarized models.
- We are filling this gap [Work in progr.], [JHEP**1811** 010], [JHEP**1811**, 010], [JHEP**1711**, 098], [Eur.Phys.J.C**77** no.7, 436], [Eur.Phys.J.C**77** no.4].
  - (Weak) couplings with other initial or final states: $\gamma\gamma$, $t\bar{t}$.
  - Developing a UFO model for MadGraph v5.
- We choose MadGraph v5 because of its *easy* interfacing with other programs in the Monte Carlo chain. Both from the analytical side (FeynRules) and on the computational one (lhapdf6, Pythia, DELPHES, ExRootAnalysis, MadAnalysis 5,...).
- But we acknowledge the big improvements of other options (like Whizard and SHERPA) on this topic.

Our approach

- We have theoretical background on comparing different unitarization procedures, and on their motivation: [Phys.Rev.Lett.**114**, 221803], [PRD**91**, 075017], [JHEP**140**, 149],...
- However, we were lacking an independent Monte Carlo implementation of the unitarized models.
- We are filling this gap [Work in progr.], [JHEP**1811** 010], [JHEP**1811**, 010], [JHEP**1711**, 098], [Eur.Phys.J.C**77** no.7, 436], [Eur.Phys.J.C**77** no.4].
    - (Weak) couplings with other initial or final states: $\gamma\gamma$, $t\bar{t}$.
    - Developing a UFO model for MadGraph v5.
- We choose MadGraph v5 because of its *easy* interfacing with other programs in the Monte Carlo chain. Both from the analytical side (FeynRules) and on the computational one (lhapdf6, Pythia, DELPHES, ExRootAnalysis, MadAnalysis 5,...).
- But we acknowledge the big improvements of other options (like Whizard and SHERPA) on this topic.

Our approach: non-linear EFT

- We are interested in the collider phenomenology of Vector Bosons Scattering (in this work, $WZ \to WZ$ and $WW \to WW$), since it is very sensitive to new physics in the EW sector in the LHC.
- Bottom to Top approach: we construct an EFT for the EW sector. $SU(2)_L \times SU(2)_R$, EChL copy of ChPT in QCD.
- Degrees of freedom: Gauge Bosons $W^\pm$, Z + Higgs sector. We do not consider fermions in this work.
- Simplif. to 4 parameters: a, b, a_4, a_5. Custodial symmetry assum.

EWChL

$$\mathcal{L}_2 = \frac{v^2}{4}\left[1 + 2a\frac{h}{v} + b\left(\frac{h}{v}\right)^2 + \dots\right]\mathrm{Tr}(D_\mu U^\dagger D_\mu U) + \frac{1}{2}\partial_\mu h \partial^\mu h + \dots$$

$$\mathcal{L}_4 = a_4[\mathrm{Tr}(V_\mu V_\nu)][\mathrm{Tr}(V^\mu V^\nu)] + a_5[\mathrm{Tr}(V_\mu V^\mu)][\mathrm{Tr}(V_\nu V^\nu)] + \dots$$

$$V_\mu = (D_\mu U)U^\dagger, \qquad U = \exp\left(\frac{i\omega^a \tau^a}{v}\right)$$

Our approach: non-linear EFT

- We are interested in the collider phenomenology of Vector Bosons Scattering (in this work, $WZ \to WZ$ and $WW \to WW$), since it is very sensitive to new physics in the EW sector in the LHC.
- Bottom to Top approach: we construct an EFT for the EW sector. $SU(2)_L \times SU(2)_R$, EChL copy of ChPT in QCD.
- Degrees of freedom: Gauge Bosons $W^{\pm}$, Z + Higgs sector. We do not consider fermions in this work.
- Simplif. to 4 parameters: a, b, a_4, a_5. Custodial symmetry assum.

EWChL

$$\mathcal{L}_2 = \frac{v^2}{4}\left[1 + 2a\frac{h}{v} + b\left(\frac{h}{v}\right)^2 + \dots\right]\mathrm{Tr}(D_\mu U^\dagger D_\mu U) + \frac{1}{2}\partial_\mu h \partial^\mu h + \dots$$

$$\mathcal{L}_4 = a_4[\mathrm{Tr}(V_\mu V_\nu)][\mathrm{Tr}(V^\mu V^\nu)] + a_5[\mathrm{Tr}(V_\mu V^\mu)][\mathrm{Tr}(V_\nu V^\nu)] + \dots$$

$$V_\mu = (D_\mu U)U^\dagger, \qquad U = \exp\left(\frac{i\omega^a \tau^a}{v}\right)$$

Our approach: non-linear EFT

- We are interested in the collider phenomenology of Vector Bosons Scattering (in this work, $WZ \to WZ$ and $WW \to WW$), since it is very sensitive to new physics in the EW sector in the LHC.
- Bottom to Top approach: we construct an EFT for the EW sector. $SU(2)_L \times SU(2)_R$, EChL copy of ChPT in QCD.
- Degrees of freedom: Gauge Bosons $W^{\pm}$, Z + Higgs sector. We do not consider fermions in this work.
- Simplif. to 4 parameters: a, b, a_4, a_5. Custodial symmetry assum.

EWChL

$$\mathcal{L}_2 = \frac{v^2}{4}\left[1 + 2a\frac{h}{v} + b\left(\frac{h}{v}\right)^2 + \ldots\right]\mathrm{Tr}(D_\mu U^\dagger D_\mu U) + \frac{1}{2}\partial_\mu h \partial^\mu h + \ldots$$

$$\mathcal{L}_4 = a_4[\mathrm{Tr}(V_\mu V_\nu)][\mathrm{Tr}(V^\mu V^\nu)] + a_5[\mathrm{Tr}(V_\mu V^\mu)][\mathrm{Tr}(V_\nu V^\nu)] + \ldots$$

$$V_\mu = (D_\mu U)U^\dagger, \qquad U = \exp\left(\frac{i\omega^a \tau^a}{v}\right)$$

Our approach: non-linear EFT

- We are interested in the collider phenomenology of Vector Bosons Scattering (in this work, $WZ \to WZ$ and $WW \to WW$), since it is very sensitive to new physics in the EW sector in the LHC.
- Bottom to Top approach: we construct an EFT for the EW sector. $SU(2)_L \times SU(2)_R$, EChL copy of ChPT in QCD.
- Degrees of freedom: Gauge Bosons $W^{\pm}$, Z + Higgs sector. We do not consider fermions in this work.
- Simplif. to 4 parameters: a, b, a_4, a_5. Custodial symmetry assum.

EWChL

$$\mathcal{L}_2 = \frac{v^2}{4}\left[1 + 2a\frac{h}{v} + b\left(\frac{h}{v}\right)^2 + \dots\right]\mathrm{Tr}(D_\mu U^\dagger D_\mu U) + \frac{1}{2}\partial_\mu h \partial^\mu h + \dots$$

$$\mathcal{L}_4 = a_4[\mathrm{Tr}(V_\mu V_\nu)][\mathrm{Tr}(V^\mu V^\nu)] + a_5[\mathrm{Tr}(V_\mu V^\mu)][\mathrm{Tr}(V_\nu V^\nu)] + \dots$$

$$V_\mu = (D_\mu U)U^\dagger, \qquad U = \exp\left(\frac{i\omega^a\tau^a}{v}\right)$$

Unitarity and Partial Waves

- The NLO-computed EFT grows with the CM energy like $A \sim s^2$. Eventually reaching the unitarity bound, becoming non-perturbative.
- Violation of unitarity of the S matrix. That is, an unphysical leak in the interaction probability among EW gauge bosons.
- Tool for studying this phenomena: partial waves.
- For $WZ \to WZ$ processes, [arXiv:1907.06668]

$$a^J_{\lambda_1\lambda_2\lambda_3\lambda_4}(s) = \frac{1}{64\pi}\int_{-1}^{1} d\,\cos\theta\, A_{W_{\lambda_1}Z_{\lambda_2}\to W_{\lambda_3}Z_{\lambda_4}}(s,\cos\theta)\, d^J_{\lambda,\lambda'}(\cos\theta),$$

J, total angular momentum; $\lambda = \lambda_1 - \lambda_2$; $\lambda' = \lambda_3 - \lambda_4$; λ_i, helicity state of the i-nth external gauge boson; $d^J_{\lambda,\lambda'}(\cos\theta)$, Wigner functions.

Unitarity and Partial Waves

- The NLO-computed EFT grows with the CM energy like $A \sim s^2$. Eventually reaching the unitarity bound, becoming non-perturbative.
- Violation of unitarity of the S matrix. That is, an unphysical leak in the interaction probability among EW gauge bosons.
- Tool for studying this phenomena: partial waves.
- For $WZ \to WZ$ processes, [arXiv:1907.06668]

$$a^J_{\lambda_1\lambda_2\lambda_3\lambda_4}(s) = \frac{1}{64\pi}\int_{-1}^{1} d\,\cos\theta\, A_{W_{\lambda_1}Z_{\lambda_2}\to W_{\lambda_3}Z_{\lambda_4}}(s,\cos\theta)\, d^J_{\lambda,\lambda'}(\cos\theta),$$

J, total angular momentum; $\lambda = \lambda_1 - \lambda_2$; $\lambda' = \lambda_3 - \lambda_4$; λ_i, helicity state of the i-nth external gauge boson; $d^J_{\lambda,\lambda'}(\cos\theta)$, Wigner functions.

Unitarity and Partial Waves

- The NLO-computed EFT grows with the CM energy like $A \sim s^2$. Eventually reaching the unitarity bound, becoming non-perturbative.
- Violation of unitarity of the S matrix. That is, an unphysical leak in the interaction probability among EW gauge bosons.
- Tool for studying this phenomena: partial waves.
- For $WZ \to WZ$ processes, [arXiv:1907.06668]

$$a^J_{\lambda_1\lambda_2\lambda_3\lambda_4}(s) = \frac{1}{64\pi}\int_{-1}^{1} d\,\cos\theta\, A_{W_{\lambda_1}Z_{\lambda_2}\to W_{\lambda_3}Z_{\lambda_4}}(s,\cos\theta)\, d^J_{\lambda,\lambda'}(\cos\theta),$$

J, total angular momentum; $\lambda = \lambda_1 - \lambda_2$; $\lambda' = \lambda_3 - \lambda_4$; λ_i, helicity state of the i-nth external gauge boson; $d^J_{\lambda,\lambda'}(\cos\theta)$, Wigner functions.

Unitarity and Partial Waves

- The NLO-computed EFT grows with the CM energy like $A \sim s^2$. Eventually reaching the unitarity bound, becoming non-perturbative.
- Violation of unitarity of the S matrix. That is, an unphysical leak in the interaction probability among EW gauge bosons.
- Tool for studying this phenomena: partial waves.
- For $WZ \to WZ$ processes, [arXiv:1907.06668]

$$a^J_{\lambda_1\lambda_2\lambda_3\lambda_4}(s) = \frac{1}{64\pi}\int_{-1}^{1} d\,\cos\theta\, A_{W_{\lambda_1}Z_{\lambda_2}\to W_{\lambda_3}Z_{\lambda_4}}(s,\cos\theta)\, d^J_{\lambda,\lambda'}(\cos\theta),$$

J, total angular momentum; $\lambda = \lambda_1 - \lambda_2$; $\lambda' = \lambda_3 - \lambda_4$; λ_i, helicity state of the i-nth external gauge boson; $d^J_{\lambda,\lambda'}(\cos\theta)$, Wigner functions.

Unitarity for generic partial waves

- Unit. cond. for $S - matrix$: $SS^\dagger = \mathbb{1}$,
- plus analytical properties of matrix elements,
- plus time reversal invariance,

Unitarity condition for partial waves

$$\mathrm{Im}\, A_{IJ,p_i\to k_1}(s) = \sum_{\{a,b\}} \sqrt{1-\frac{4m_q^2}{s}}[A_{IJ,p_i\to q_{i,ab}}(s)][A_{IJ,q_{i,ab}\to k_i}(s)]^*$$

Unitarity for generic partial waves

- Unit. cond. for $S - matrix$: $SS^\dagger = \mathbb{1}$,
- plus analytical properties of matrix elements,
- plus time reversal invariance,

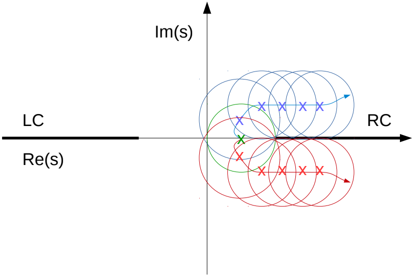

Unitarity condition for partial waves

$$\mathrm{Im}\, A_{IJ,p_i\to k_1}(s) = \sum_{\{a,b\}} \sqrt{1-\frac{4m_q^2}{s}}\,[A_{IJ,p_i\to q_{i,ab}}(s)][A_{IJ,q_{i,ab}\to k_i}(s)]^*$$

Unitarity for generic partial waves

- Unit. cond. for $S - matrix$: $SS^\dagger = \mathbb{1}$,
- plus analytical properties of matrix elements,
- plus time reversal invariance,

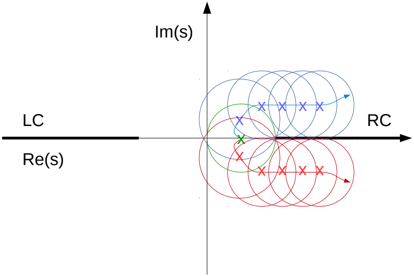

Unitarity condition for partial waves

$$\mathrm{Im}\, A_{IJ,p_i\rightarrow k_1}(s) = \sum_{\{a,b\}} \sqrt{1-\frac{4m_q^2}{s}} [A_{IJ,p_i\rightarrow q_{i,ab}}(s)][A_{IJ,q_{i,ab}\rightarrow k_i}(s)]^*$$

Unitarity for generic partial waves

- Unit. cond. for $S - matrix$: $SS^\dagger = \mathbb{1}$,
- plus analytical properties of matrix elements,
- plus time reversal invariance,

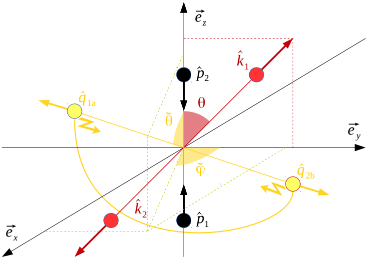

Unitarity condition for partial waves

$$\mathrm{Im}\, A_{IJ,p_i\to k_1}(s) = \sum_{\{a,b\}} \sqrt{1-\frac{4m_q^2}{s}}[A_{IJ,p_i\to q_{i,ab}}(s)][A_{IJ,q_{i,ab}\to k_i}(s)]^*$$

Unitarity for $WZ \to WZ$ Partial Waves

- Unitarity requires

$$\mathrm{Im}[a^J_{\lambda_1\lambda_2\lambda_3\lambda_4}(s)] = |a^J_{\lambda_1\lambda_2\lambda_3\lambda_4}(s)|^2 = \sum_{\lambda_a,\lambda_b,\lambda_c,\lambda_d} [a^J_{\lambda_1\lambda_2\lambda_a\lambda_b}(s)][a^J_{\lambda_c\lambda_d\lambda_3\lambda_4}(s)]^*$$

- Note that partial waves $a^J_{\lambda.,\lambda.,\lambda.,\lambda.}(s)$ carry the $d^J_{\lambda,\lambda'}(\cos\theta)$ Wigner functions. These stands for the algebra of polarization vectors λ_i $(i = a, b, c, d)$ of *internal* WZ states.
- Unitarity expression can be rewritten as

$$|a^J(s)| \leq 1.$$

- Because $a^J(s)$ scales with $\mathcal{O}(s^n)$ on EFT approach, such an expression allows us to compute a maximum energy scale after which the *raw* EFT breaks.

Unitarity for $WZ \to WZ$ Partial Waves

- Unitarity requires

$$\mathrm{Im}[a^J_{\lambda_1\lambda_2\lambda_3\lambda_4}(s)] = |a^J_{\lambda_1\lambda_2\lambda_3\lambda_4}(s)|^2 = \sum_{\lambda_a,\lambda_b,\lambda_c,\lambda_d} [a^J_{\lambda_1\lambda_2\lambda_a\lambda_b}(s)][a^J_{\lambda_c\lambda_d\lambda_3\lambda_4}(s)]^*$$

- Note that partial waves $a^J_{\lambda_\cdot,\lambda_\cdot,\lambda_\cdot,\lambda_\cdot}(s)$ carry the $d^J_{\lambda,\lambda'}(\cos\theta)$ Wigner functions. These stands for the algebra of polarization vectors λ_i $(i = a, b, c, d)$ of *internal* WZ states.
- Unitarity expression can be rewritten as

$$|a^J(s)| \leq 1.$$

- Because $a^J(s)$ scales with $\mathcal{O}(s^n)$ on EFT approach, such an expression allows us to compute a maximum energy scale after which the *raw* EFT breaks.

Unitarity for $WZ \to WZ$ Partial Waves

- Unitarity requires

$$\mathrm{Im}[a^J_{\lambda_1\lambda_2\lambda_3\lambda_4}(s)] = |a^J_{\lambda_1\lambda_2\lambda_3\lambda_4}(s)|^2 = \sum_{\lambda_a,\lambda_b,\lambda_c,\lambda_d} [a^J_{\lambda_1\lambda_2\lambda_a\lambda_b}(s)][a^J_{\lambda_c\lambda_d\lambda_3\lambda_4}(s)]^*$$

- Note that partial waves $a^J_{\lambda.,\lambda.,\lambda.,\lambda.}(s)$ carry the $d^J_{\lambda,\lambda'}(\cos\theta)$ Wigner functions. These stands for the algebra of polarization vectors λ_i $(i = a, b, c, d)$ of *internal* WZ states.
- Unitarity expression can be rewritten as

$$|a^J(s)| \leq 1.$$

- Because $a^J(s)$ scales with $\mathcal{O}(s^n)$ on EFT approach, such an expression allows us to compute a maximum energy scale after which the *raw* EFT breaks.

Unitarity for $WZ \to WZ$ Partial Waves

- Unitarity requires

$$\mathrm{Im}[a^J_{\lambda_1\lambda_2\lambda_3\lambda_4}(s)] = |a^J_{\lambda_1\lambda_2\lambda_3\lambda_4}(s)|^2 = \sum_{\lambda_a,\lambda_b,\lambda_c,\lambda_d} [a^J_{\lambda_1\lambda_2\lambda_a\lambda_b}(s)][a^J_{\lambda_c\lambda_d\lambda_3\lambda_4}(s)]^*$$

- Note that partial waves $a^J_{\lambda.,\lambda.,\lambda.,\lambda.}(s)$ carry the $d^J_{\lambda,\lambda'}(\cos\theta)$ Wigner functions. These stands for the algebra of polarization vectors λ_i $(i = a, b, c, d)$ of *internal* WZ states.
- Unitarity expression can be rewritten as

$$|a^J(s)| \leq 1.$$

- Because $a^J(s)$ scales with $\mathcal{O}(s^n)$ on EFT approach, such an expression allows us to compute a maximum energy scale after which the *raw* EFT breaks.

Unitarity for $WZ \to WZ$ Partial Waves

- The NLO-computed EFT grows with the CM energy like $A \sim s^2$. Hence, it will eventually reach the unitarity bound, becoming non-perturbative. Options:
- **Cut-Off**: limit the validity range of the EFT to the perturbative region to the minimum value of s that saturates $|a^J(s)| = 1$. The EFT is considered as a useful parameterization of slight deviations from the SM in the range under the TeV scale.
- **Form Factor (FF)**: instead of obviating part of the raw EFT results, suppress the pathological behaviour via multiplying the partial wave by a smooth, continuous function

$$f_i^{\mathrm{FF}} = (1 + s/\Lambda_i^2)^{-\varepsilon_i},$$

where Λ_i^2 is the minimum value of s that breaks unitarity in channel i and ε_i, the minimum exponent that fixes the pathological behaviour.

Unitarity for $WZ \to WZ$ Partial Waves

- The NLO-computed EFT grows with the CM energy like $A \sim s^2$. Hence, it will eventually reach the unitarity bound, becoming non-perturbative. Options:
- **Cut-Off**: limit the validity range of the EFT to the perturbative region to the minimum value of s that saturates $|a^J(s)| = 1$. The EFT is considered as a useful parameterization of slight deviations from the SM in the range under the TeV scale.
- **Form Factor (FF)**: instead of obviating part of the raw EFT results, suppress the pathological behaviour via multiplying the partial wave by a smooth, continuous function

$$f_i^{\mathrm{FF}} = (1 + s/\Lambda_i^2)^{-\varepsilon_i},$$

where Λ_i^2 is the minimum value of s that breaks unitarity in channel i and ε_i, the minimum exponent that fixes the pathological behaviour.

Unitarity for $WZ \to WZ$ Partial Waves

- The NLO-computed EFT grows with the CM energy like $A \sim s^2$. Hence, it will eventually reach the unitarity bound, becoming non-perturbative. Options:
- **Cut-Off**: limit the validity range of the EFT to the perturbative region to the minimum value of s that saturates $|a^J(s)| = 1$. The EFT is considered as a useful parameterization of slight deviations from the SM in the range under the TeV scale.
- **Form Factor (FF)**: instead of obviating part of the raw EFT results, suppress the pathological behaviour via multiplying the partial wave by a smooth, continuous function

  $$f_i^{\mathrm{FF}} = (1 + s/\Lambda_i^2)^{-\varepsilon_i},$$

  where Λ_i^2 is the minimum value of s that breaks unitarity in channel i and ε_i, the minimum exponent that fixes the pathological behaviour.

Unitarity for $WZ \to WZ$ Partial Waves

- **Kink**: similar to the FF approach. The main difference is that the suppression is not smooth, but through a step function

$$f_i^{\mathrm{Kink}} = \begin{cases} 1, & \text{if } s \leq \Lambda_i^2 \\ (s/\Lambda_i^2)^{-\varepsilon_i}, & \text{if } s > \Lambda_i^2 \end{cases}$$

- **Take advantage of the analytical properties of the S-Matrix**, encoded inside dispersion relations and unitar. proced., to study the non-perturbative region (TeV scale) of the theory. This is a theoretically motivated extension of the EFT.
- Different unitarization procedures have been proposed: K-Matrix, T-Matrix, N/D, IAM,...
- An extensive analysis has been carried out in [PRD**91**, 075017].

Unitarity for $WZ \to WZ$ Partial Waves

- **Kink**: similar to the FF approach. The main difference is that the suppression is not smooth, but through a step function

$$f_i^{\mathrm{Kink}} = \begin{cases} 1, & \text{if } s \leq \Lambda_i^2 \\ (s/\Lambda_i^2)^{-\varepsilon_i}, & \text{if } s > \Lambda_i^2 \end{cases}$$

- **Take advantage of the analytical properties of the S-Matrix**, encoded inside dispersion relations and unitar. proced., to study the non-perturbative region (TeV scale) of the theory. This is a theoretically motivated extension of the EFT.
- Different unitarization procedures have been proposed: K-Matrix, T-Matrix, N/D, IAM,...
- An extensive analysis has been carried out in [PRD**91**, 075017].

Unitarity for $WZ \to WZ$ Partial Waves

- **Kink**: similar to the FF approach. The main difference is that the suppression is not smooth, but through a step function

$$f_i^{\mathrm{Kink}} = \begin{cases} 1, & \text{if } s \leq \Lambda_i^2 \\ (s/\Lambda_i^2)^{-\varepsilon_i}, & \text{if } s > \Lambda_i^2 \end{cases}$$

- **Take advantage of the analytical properties of the S-Matrix**, encoded inside dispersion relations and unitar. proced., to study the non-perturbative region (TeV scale) of the theory. This is a theoretically motivated extension of the EFT.
- Different unitarization procedures have been proposed: K-Matrix, T-Matrix, N/D, IAM,...
- An extensive analysis has been carried out in [PRD**91**, 075017].

Unitarity for $WZ \to WZ$ Partial Waves

- **Kink**: similar to the FF approach. The main difference is that the suppression is not smooth, but through a step function

$$f_i^{\mathrm{Kink}} = \begin{cases} 1, & \text{if } s \leq \Lambda_i^2 \\ (s/\Lambda_i^2)^{-\varepsilon_i}, & \text{if } s > \Lambda_i^2 \end{cases}$$

- **Take advantage of the analytical properties of the S-Matrix**, encoded inside dispersion relations and unitar. proced., to study the non-perturbative region (TeV scale) of the theory. This is a theoretically motivated extension of the EFT.
- Different unitarization procedures have been proposed: K-Matrix, T-Matrix, N/D, IAM,...
- An extensive analysis has been carried out in [PRD**91**, 075017].

Unitarization procedures for elastic processes, generic $\omega\omega \to \omega\omega$

$$A^{IAM}(s) = \frac{[A^{(0)}(s)]^2}{A^{(0)}(s) - A^{(1)}(s)},$$

$$A^{N/D}(s) = \frac{A^{(0)}(s) + A_L(s)}{1 - \frac{A_R(s)}{A^{(0)}(s)} + \frac{1}{2}g(s)A_L(-s)},$$

$$A^{IK}(s) = \frac{A^{(0)}(s) + A_L(s)}{1 - \frac{A_R(s)}{A^{(0)}(s)} + g(s)A_L(s)},$$

$$A_0^K(s) = \frac{A_0(s)}{1 - iA_0(s)},$$

where

$$g(s) = \frac{1}{\pi}\left(\frac{B(\mu)}{D+E} + \log\frac{-s}{\mu^2}\right)$$

$$A_L(s) = \pi g(-s) D s^2$$

$$A_R(s) = \pi g(s) E s^2$$

PRD **91** (2015) 075017

Unitarization procedures for elastic processes, generic $\omega\omega \to \omega\omega$

$$A^{IAM}(s) = \frac{[A^{(0)}(s)]^2}{A^{(0)}(s) - A^{(1)}(s)},$$

$$A^{N/D}(s) = \frac{A^{(0)}(s) + A_L(s)}{1 - \frac{A_R(s)}{A^{(0)}(s)} + \frac{1}{2}g(s)A_L(-s)},$$

$$A^{IK}(s) = \frac{A^{(0)}(s) + A_L(s)}{1 - \frac{A_R(s)}{A^{(0)}(s)} + g(s)A_L(s)},$$

$$A_0^K(s) = \frac{A_0(s)}{1 - iA_0(s)},$$

where

$$g(s) = \frac{1}{\pi}\left(\frac{B(\mu)}{D+E} + \log\frac{-s}{\mu^2}\right)$$

$$A_L(s) = \pi g(-s) D s^2$$

$$A_R(s) = \pi g(s) E s^2$$

PRD **91** (2015) 075017

Unitarization procedures for elastic processes, generic $\omega\omega \to \omega\omega$

$$A^{IAM}(s) = \frac{[A^{(0)}(s)]^2}{A^{(0)}(s) - A^{(1)}(s)},$$

$$A^{N/D}(s) = \frac{A^{(0)}(s) + A_L(s)}{1 - \frac{A_R(s)}{A^{(0)}(s)} + \frac{1}{2} g(s) A_L(-s)},$$

$$A^{IK}(s) = \frac{A^{(0)}(s) + A_L(s)}{1 - \frac{A_R(s)}{A^{(0)}(s)} + g(s) A_L(s)},$$

$$A_0^K(s) = \frac{A_0(s)}{1 - iA_0(s)},$$

where

$$g(s) = \frac{1}{\pi}\left(\frac{B(\mu)}{D+E} + \log\frac{-s}{\mu^2}\right)$$

$$A_L(s) = \pi g(-s) D s^2$$

$$A_R(s) = \pi g(s) E s^2$$

PRD **91** (2015) 075017

Unitarization procedures for elastic processes, generic $\omega\omega \to \omega\omega$

$$A^{IAM}(s) = \frac{[A^{(0)}(s)]^2}{A^{(0)}(s) - A^{(1)}(s)},$$

$$A^{N/D}(s) = \frac{A^{(0)}(s) + A_L(s)}{1 - \frac{A_R(s)}{A^{(0)}(s)} + \frac{1}{2}g(s)A_L(-s)},$$

$$A^{IK}(s) = \frac{A^{(0)}(s) + A_L(s)}{1 - \frac{A_R(s)}{A^{(0)}(s)} + g(s)A_L(s)},$$

$$A_0^K(s) = \frac{A_0(s)}{1 - iA_0(s)},$$

where

$$g(s) = \frac{1}{\pi}\left(\frac{B(\mu)}{D+E} + \log\frac{-s}{\mu^2}\right)$$

$$A_L(s) = \pi g(-s)Ds^2$$

$$A_R(s) = \pi g(s)Es^2$$

PRD **91** (2015) 075017

Matricial versions of the methods, generic $\omega\omega \to \omega\omega$

$$F^{IAM}(s) = \left[F^{(0)}(s)\right]^{-1} \cdot \left[F^{(0)}(s) - F^{(1)}(s)\right] \cdot \left[F^{(0)}(s)\right]^{-1},$$

$$F^{N/D}(s) = \left[1 - F_R(s) \cdot \left(F^{(0)}(s)\right)^{-1} + \frac{1}{2} G(s) F_L(-s)\right]^{-1} \cdot N_0(s),$$

$$F^{IK}(s) = [1 + G(s) \cdot N_0(s)]^{-1} \cdot N_0(s),$$

where $G(s)$, $F_L(s)$, $F_R(s)$ and $N_0(s)$ are defined as

$$G(s) = \frac{1}{\pi}\left(B(\mu)(D+E)^{-1} + \log\frac{-s}{\mu^2}\right)$$

$$F_L(s) = \pi G(-s) D s^2$$

$$F_R(s) = \pi G(s) E s^2$$

$$N_0(s) = F^{(0)}(s) + F_L(s)$$

PRD **91** (2015) 075017

Matricial versions of the methods, generic $\omega\omega \to \omega\omega$

$$F^{IAM}(s) = \left[F^{(0)}(s)\right]^{-1} \cdot \left[F^{(0)}(s) - F^{(1)}(s)\right] \cdot \left[F^{(0)}(s)\right]^{-1},$$

$$F^{N/D}(s) = \left[1 - F_R(s) \cdot \left(F^{(0)}(s)\right)^{-1} + \frac{1}{2} G(s) F_L(-s)\right]^{-1} \cdot N_0(s),$$

$$F^{IK}(s) = [1 + G(s) \cdot N_0(s)]^{-1} \cdot N_0(s),$$

where $G(s)$, $F_L(s)$, $F_R(s)$ and $N_0(s)$ are defined as

$$G(s) = \frac{1}{\pi}\left(B(\mu)(D+E)^{-1} + \log\frac{-s}{\mu^2}\right)$$

$$F_L(s) = \pi G(-s) D s^2$$

$$F_R(s) = \pi G(s) E s^2$$

$$N_0(s) = F^{(0)}(s) + F_L(s)$$

PRD **91** (2015) 075017

Matricial versions of the methods, generic $\omega\omega \to \omega\omega$

$$F^{IAM}(s) = \left[F^{(0)}(s)\right]^{-1} \cdot \left[F^{(0)}(s) - F^{(1)}(s)\right] \cdot \left[F^{(0)}(s)\right]^{-1},$$

$$F^{N/D}(s) = \left[1 - F_R(s) \cdot \left(F^{(0)}(s)\right)^{-1} + \frac{1}{2} G(s) F_L(-s)\right]^{-1} \cdot N_0(s),$$

$$F^{IK}(s) = [1 + G(s) \cdot N_0(s)]^{-1} \cdot N_0(s),$$

where $G(s)$, $F_L(s)$, $F_R(s)$ and $N_0(s)$ are defined as

$$G(s) = \frac{1}{\pi}\left(B(\mu)(D+E)^{-1} + \log\frac{-s}{\mu^2}\right)$$

$$F_L(s) = \pi G(-s) D s^2$$

$$F_R(s) = \pi G(s) E s^2$$

$$N_0(s) = F^{(0)}(s) + F_L(s)$$

PRD **91** (2015) 075017

Usability channel of unitarization procedures, generic

$\omega\omega \to \omega\omega$

IJ	00	02	11	20	22
Method of choice	Any	N/D IK	IAM	Any	N/D IK

- The IAM method cannot be used when $A^{(0)} = 0$, because it would give a vanishing value.
- The N/D and the IK methods cannot be used if $D + E = 0$, because in this case computing $A_L(s)$ and $A_R(s)$ is not possible.
- The naive K-matrix method,

$$A_0^K(s) = \frac{A_0(s)}{1 - iA_0(s)},$$

  fails because it is not analytical in the first Riemann sheet and, consequently, it is not a proper partial wave compatible with microcausality.

Usability channel of unitarization procedures, generic $\omega\omega \to \omega\omega$

IJ	00	02	11	20	22
Method of choice	Any	N/D IK	IAM	Any	N/D IK

- The IAM method cannot be used when $A^{(0)} = 0$, because it would give a vanishing value.
- The N/D and the IK methods cannot be used if $D + E = 0$, because in this case computing $A_L(s)$ and $A_R(s)$ is not possible.
- The naive K-matrix method,

$$A_0^K(s) = \frac{A_0(s)}{1 - iA_0(s)},$$

fails because it is not analytical in the first Riemann sheet and, consequently, it is not a proper partial wave compatible with microcausality.

Usability channel of unitarization procedures, generic $\omega\omega \to \omega\omega$

IJ	00	02	11	20	22
Method of choice	Any	N/D IK	IAM	Any	N/D IK

- The IAM method cannot be used when $A^{(0)} = 0$, because it would give a vanishing value.
- The N/D and the IK methods cannot be used if $D + E = 0$, because in this case computing $A_L(s)$ and $A_R(s)$ is not possible.
- The naive K-matrix method,

$$A_0^K(s) = \frac{A_0(s)}{1 - iA_0(s)},$$

fails because it is not analytical in the first Riemann sheet and, consequently, it is not a proper partial wave compatible with microcausality.

K-Matrix, $WZ \to WZ$, $J = 1$

$$a^{J;\mathrm{K-Matrix}}(s) = \frac{a^J(s)}{1 - i a^J(s)}$$

- It has been extensively used in ChPT in QCD. It is a prescription applied to the partial wave amplitudes and basically projects the non-unitary ones into the Argand circle through a stereographic projection.
- It takes a real, non unitary partial wave amplitude to which an imaginary part is added ad hoc such that the uni- tarity limit is saturated.
- It breaks some of the analytical properties of the S-matrix (poles in the first Riemann sheet).
- Updated to T-Matrix.

K-Matrix, $WZ \to WZ$, $J = 1$

$$a^{J;\mathrm{K-Matrix}}(s) = \frac{a^J(s)}{1 - i a^J(s)}$$

- It has been extensively used in ChPT in QCD. It is a prescription applied to the partial wave amplitudes and basically projects the non-unitary ones into the Argand circle through a stereographic projection.
- It takes a real, non unitary partial wave amplitude to which an imaginary part is added ad hoc such that the uni- tarity limit is saturated.
- It breaks some of the analytical properties of the S-matrix (poles in the first Riemann sheet).
- Updated to **T-Matrix**.

K-Matrix, $WZ \to WZ$, $J = 1$

$$a^{J;\mathrm{K-Matrix}}(s) = \frac{a^J(s)}{1 - ia^J(s)}$$

- It has been extensively used in ChPT in QCD. It is a prescription applied to the partial wave amplitudes and basically projects the non-unitary ones into the Argand circle through a stereographic projection.
- It takes a real, non unitary partial wave amplitude to which an imaginary part is added ad hoc such that the uni- tarity limit is saturated.
- It breaks some of the analytical properties of the S-matrix (poles in the first Riemann sheet).
- Updated to **T-Matrix**.

K-Matrix, $WZ \to WZ$, $J = 1$

$$a^{J;\mathrm{K-Matrix}}(s) = \frac{a^J(s)}{1 - i a^J(s)}$$

- It has been extensively used in ChPT in QCD. It is a prescription applied to the partial wave amplitudes and basically projects the non-unitary ones into the Argand circle through a stereographic projection.
- It takes a real, non unitary partial wave amplitude to which an imaginary part is added ad hoc such that the uni- tarity limit is saturated.
- It breaks some of the analytical properties of the S-matrix (poles in the first Riemann sheet).
- Updated to **T-Matrix**.

K-Matrix, $WZ \to WZ$, $J = 1$

$$a^{J;\mathrm{K-Matrix}}(s) = \frac{a^J(s)}{1 - ia^J(s)}$$

- It has been extensively used in ChPT in QCD. It is a prescription applied to the partial wave amplitudes and basically projects the non-unitary ones into the Argand circle through a stereographic projection.
- It takes a real, non unitary partial wave amplitude to which an imaginary part is added ad hoc such that the uni- tarity limit is saturated.
- It breaks some of the analytical properties of the S-matrix (poles in the first Riemann sheet).
- Updated to **T-Matrix**.

Inverse Amplitude Method (IAM), $WZ \to WZ$, $J = 1$

$$a^{J;\mathrm{IAM}}(s) = \frac{[a^{J;(2)}(s)]^2}{A^{J;(2)}(s) - A^{J;(4)}(s)}$$

- It is based on dispersion relations. The partial wave a^J is decomposed into two contributions in the chiral expansion, one of order $\mathcal{O}(p^2)$ and the other one of order $\mathcal{O}(p^4)$.
- With the IAM, we dinamically generate the resonances in VBS.
- In particular, the V^+, V^-, V^0 isovector resonances ($J = 1$).

Inverse Amplitude Method (IAM), $WZ \to WZ$, $J = 1$

$$a^{J;\mathrm{IAM}}(s) = \frac{[a^{J;(2)}(s)]^2}{A^{J;(2)}(s) - A^{J;(4)}(s)}$$

- It is based on dispersion relations. The partial wave a^J is decomposed into two contributions in the chiral expansion, one of order $\mathcal{O}(p^2)$ and the other one of order $\mathcal{O}(p^4)$.
- With the IAM, we dinamically generate the resonances in VBS.
- In particular, the V^+, V^-, V^0 isovector resonances ($J = 1$).

Inverse Amplitude Method (IAM), $WZ \to WZ$, $J = 1$

$$a^{J;\mathrm{IAM}}(s) = \frac{[a^{J;(2)}(s)]^2}{A^{J;(2)}(s) - A^{J;(4)}(s)}$$

- It is based on dispersion relations. The partial wave a^J is decomposed into two contributions in the chiral expansion, one of order $\mathcal{O}(p^2)$ and the other one of order $\mathcal{O}(p^4)$.
- With the IAM, we dinamically generate the resonances in VBS.
- In particular, the V^+, V^-, V^0 isovector resonances ($J = 1$).

Inverse Amplitude Method (IAM), $WZ \to WZ$, $J = 1$

$$a^{J;\mathrm{IAM}}(s) = \frac{[a^{J;(2)}(s)]^2}{A^{J;(2)}(s) - A^{J;(4)}(s)}$$

- It is based on dispersion relations. The partial wave a^J is decomposed into two contributions in the chiral expansion, one of order $\mathcal{O}(p^2)$ and the other one of order $\mathcal{O}(p^4)$.
- With the IAM, we dinamically generate the resonances in VBS.
- In particular, the V^+, V^-, V^0 isovector resonances ($J = 1$).

Partial waves for angular momentums and helicity combinations

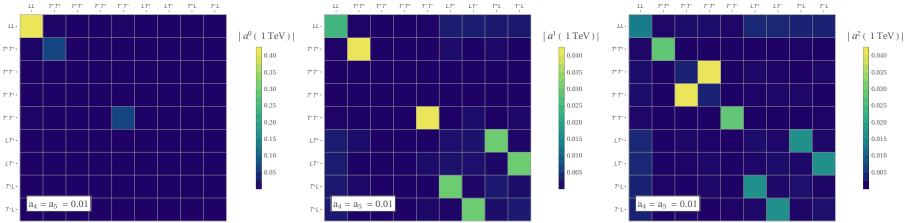

$a^J(\sqrt{s})$ with $J = 0$ (left), $J = 1$ (middle), and $J = 2$ (right), of the 81 helicity combinations of $W^+Z \to W^+Z.\sqrt{s_{WZ}} = 1\,\mathrm{TeV}$ and $a_4 = a_5 = 0.01$ (other parameters set to SM). Incoming and outgoing states can be interpreted indistinctly due to time-reversal invariance. 9 incoming WZ and 9 outgoing WZ states with two polarized gauge bosons, longitudinal (L) and/or transverse ($T^{+,-}$), denoted by: LL, T^+T^+, T^+T^-, T^-T^+ , T^-T^-, LT^+, LT^-, T^+L and T^-L.

Total cross section

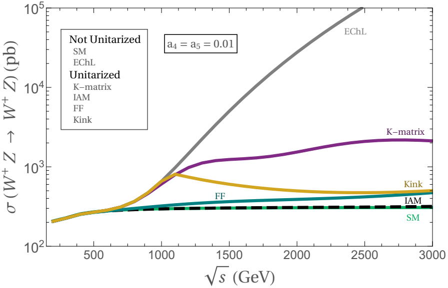

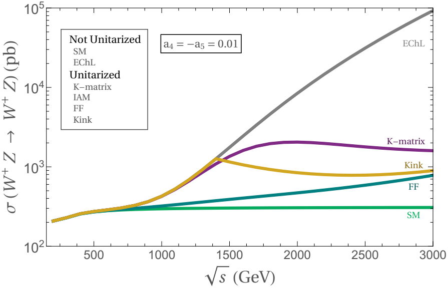

Total cross section of $W^+Z \to W^+Z$ for: K matrix (purple), Kink (yellow), FF (blue) and IAM (dashed black), Non-unitarized EChL and SM are also displayed. Two benchmark: $a_4 = a_5 = 0.01$ (left) and $a_4 = -a_5 = 0.01$ (right). In all plots $a = 1$ (or, equivalently, $\Delta a = 0$).

Total cross section

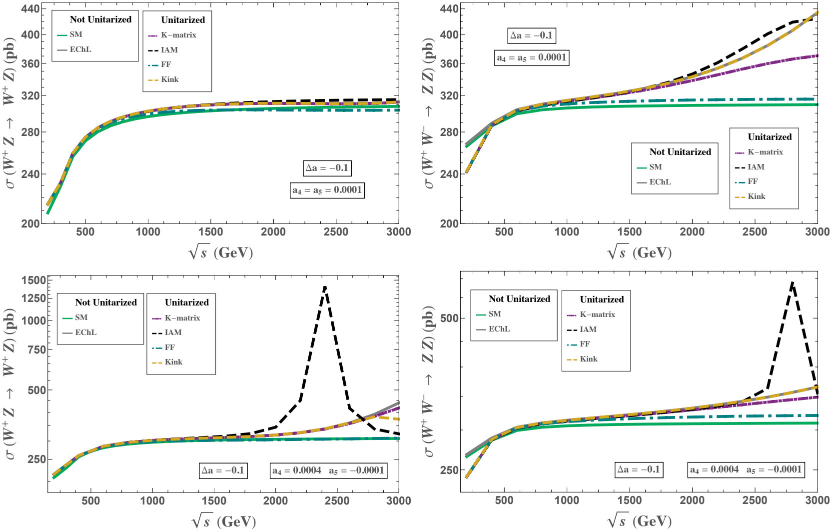

Total cross section $WZ \to WZ$ (left panels). Channel $WW \to ZZ$ (right panels). $a = 0.9$

95% confidence level exclusion in $[a_4, a_5]$, WZ final state

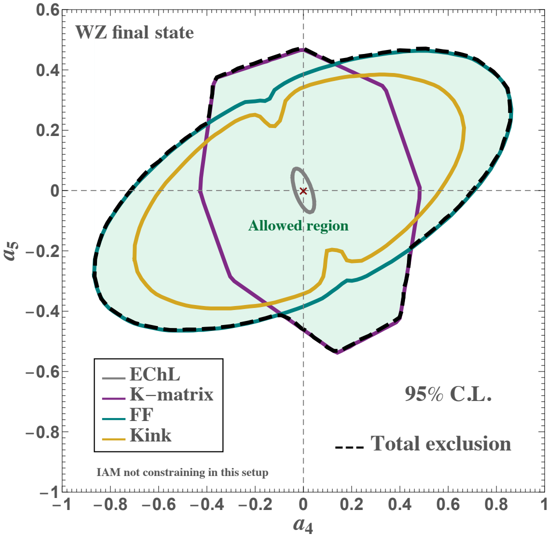

Exclusion in $[a_4, a_5]$, WZ final state at the LHC with $\sqrt{s} = 8$ TeV. Total overall exclusion region.

Conclusions

- VBS by means of the Electroweak Chiral Lagrangian and several unitarization procedures.
- The Electroweak Chiral Lagrangian is chosen because it is more suitable for strongly interacting scenarios.
- EFTs, typically, suffer from unitarity violation issues, because of the underlying structure (bounded to specific energy scales!!).
- Reliable, unitary predictions are needed to interpret experimental data.
- Option: cut-off.
- Option: ad-hoc form-factor: FF, Kint.
- Option: take advantage of mathematical properties of the S-Matrix (unitarization).
- There is a **theoretical uncertainty** in the experimental determination of effective theory parameters due to the unitarization scheme choice.
- For the IAM, $M(V^0, V^\pm)$ and $\Gamma(V^0, V^\pm)$, functions of the Chiral parameters (low energy EWChL). **NOT independent parameters**.

Conclusions

- VBS by means of the Electroweak Chiral Lagrangian and several unitarization procedures.
- The Electroweak Chiral Lagrangian is chosen because it is more suitable for strongly interacting scenarios.
- EFTs, typically, suffer from unitarity violation issues, because of the underlying structure (bounded to specific energy scales!!).
- Reliable, unitary predictions are needed to interpret experimental data.
- Option: cut-off.
- Option: ad-hoc form-factor: FF, Kint.
- Option: take advantage of mathematical properties of the S-Matrix (unitarization).
- There is a **theoretical uncertainty** in the experimental determination of effective theory parameters due to the unitarization scheme choice.
- For the IAM, $M(V^0, V^\pm)$ and $\Gamma(V^0, V^\pm)$, functions of the Chiral parameters (low energy EWChL). **NOT independent parameters**.

Conclusions

- VBS by means of the Electroweak Chiral Lagrangian and several unitarization procedures.
- The Electroweak Chiral Lagrangian is chosen because it is more suitable for strongly interacting scenarios.
- EFTs, typically, suffer from unitarity violation issues, because of the underlying structure (bounded to specific energy scales!!).
- Reliable, unitary predictions are needed to interpret experimental data.
- Option: cut-off.
- Option: ad-hoc form-factor: FF, Kint.
- Option: take advantage of mathematical properties of the S-Matrix (unitarization).
- There is a **theoretical uncertainty** in the experimental determination of effective theory parameters due to the unitarization scheme choice.
- For the IAM, $M(V^0, V^\pm)$ and $\Gamma(V^0, V^\pm)$, functions of the Chiral parameters (low energy EWChL). **NOT independent parameters**.

Conclusions

- VBS by means of the Electroweak Chiral Lagrangian and several unitarization procedures.
- The Electroweak Chiral Lagrangian is chosen because it is more suitable for strongly interacting scenarios.
- EFTs, typically, suffer from unitarity violation issues, because of the underlying structure (bounded to specific energy scales!!).
- Reliable, unitary predictions are needed to interpret experimental data.
- Option: cut-off.
- Option: ad-hoc form-factor: FF, Kint.
- Option: take advantage of mathematical properties of the S-Matrix (unitarization).
- There is a **theoretical uncertainty** in the experimental determination of effective theory parameters due to the unitarization scheme choice.
- For the IAM, $M(V^0, V^\pm)$ and $\Gamma(V^0, V^\pm)$, functions of the Chiral parameters (low energy EWChL). **NOT independent parameters**.

Conclusions

- VBS by means of the Electroweak Chiral Lagrangian and several unitarization procedures.
- The Electroweak Chiral Lagrangian is chosen because it is more suitable for strongly interacting scenarios.
- EFTs, typically, suffer from unitarity violation issues, because of the underlying structure (bounded to specific energy scales!!).
- Reliable, unitary predictions are needed to interpret experimental data.
- Option: cut-off.
- Option: ad-hoc form-factor: FF, Kint.
- Option: take advantage of mathematical properties of the S-Matrix (unitarization).
- There is a **theoretical uncertainty** in the experimental determination of effective theory parameters due to the unitarization scheme choice.
- For the IAM, $M(V^0, V^\pm)$ and $\Gamma(V^0, V^\pm)$, functions of the Chiral parameters (low energy EWChL). **NOT independent parameters**.

Conclusions

- VBS by means of the Electroweak Chiral Lagrangian and several unitarization procedures.
- The Electroweak Chiral Lagrangian is chosen because it is more suitable for strongly interacting scenarios.
- EFTs, typically, suffer from unitarity violation issues, because of the underlying structure (bounded to specific energy scales!!).
- Reliable, unitary predictions are needed to interpret experimental data.
- Option: cut-off.
- Option: ad-hoc form-factor: FF, Kint.
- Option: take advantage of mathematical properties of the S-Matrix (unitarization).
- There is a **theoretical uncertainty** in the experimental determination of effective theory parameters due to the unitarization scheme choice.
- For the IAM, $M(V^0, V^\pm)$ and $\Gamma(V^0, V^\pm)$, functions of the Chiral parameters (low energy EWChL). **NOT independent parameters**.

Conclusions

- VBS by means of the Electroweak Chiral Lagrangian and several unitarization procedures.
- The Electroweak Chiral Lagrangian is chosen because it is more suitable for strongly interacting scenarios.
- EFTs, typically, suffer from unitarity violation issues, because of the underlying structure (bounded to specific energy scales!!).
- Reliable, unitary predictions are needed to interpret experimental data.
- Option: cut-off.
- Option: ad-hoc form-factor: FF, Kint.
- Option: take advantage of mathematical properties of the S-Matrix (unitarization).
- There is a **theoretical uncertainty** in the experimental determination of effective theory parameters due to the unitarization scheme choice.
- For the IAM, $M(V^0, V^\pm)$ and $\Gamma(V^0, V^\pm)$, functions of the Chiral parameters (low energy EWChL). **NOT independent parameters**.

Conclusions

- VBS by means of the Electroweak Chiral Lagrangian and several unitarization procedures.
- The Electroweak Chiral Lagrangian is chosen because it is more suitable for strongly interacting scenarios.
- EFTs, typically, suffer from unitarity violation issues, because of the underlying structure (bounded to specific energy scales!!).
- Reliable, unitary predictions are needed to interpret experimental data.
- Option: cut-off.
- Option: ad-hoc form-factor: FF, Kint.
- Option: take advantage of mathematical properties of the S-Matrix (unitarization).
- There is a **theoretical uncertainty** in the experimental determination of effective theory parameters due to the unitarization scheme choice.
- For the IAM, $M(V^0, V^\pm)$ and $\Gamma(V^0, V^\pm)$, functions of the Chiral parameters (low energy EWChL). **NOT independent parameters**.

Conclusions

- VBS by means of the Electroweak Chiral Lagrangian and several unitarization procedures.
- The Electroweak Chiral Lagrangian is chosen because it is more suitable for strongly interacting scenarios.
- EFTs, typically, suffer from unitarity violation issues, because of the underlying structure (bounded to specific energy scales!!).
- Reliable, unitary predictions are needed to interpret experimental data.
- Option: cut-off.
- Option: ad-hoc form-factor: FF, Kint.
- Option: take advantage of mathematical properties of the S-Matrix (unitarization).
- There is a **theoretical uncertainty** in the experimental determination of effective theory parameters due to the unitarization scheme choice.
- For the IAM, $M(V^0, V^\pm)$ and $\Gamma(V^0, V^\pm)$, functions of the Chiral parameters (low energy EWChL). **NOT independent parameters**.

BACKUP SLIDES

Isovector Resonance, $V^{\pm}$, V^0 [JHEP**1711**, 098]

BP	$M_V(\mathrm{GeV})$	$\Gamma_V(\mathrm{GeV})$	$g_V(M_V^2)$	a	$a_4 \cdot 10^4$	$a_5 \cdot 10^4$
BP1	1476	14	0.033	1	3.5	-3
BP2	2039	21	0.018	1	1	-1
BP3	2472	27	0.013	1	0.5	-0.5
BP1'	1479	42	0.058	0.9	9.5	-6.5
BP2'	1980	97	0.042	0.9	5.5	-2.5
BP3'	2480	183	0.033	0.9	4	-1

These BPs have been selected for vector resonances emerging at mass M_V and width Γ_V values that are of phenomenological interest for the LHC. **Note that M_V, Γ_V and $g_V(M_V^2)$ are extracted from the EFT parameters $b = a^2$, a_4 and a_5.**

Our EFT approach for Monte Carlo: Effective Proca Lagrangian

- We are using the Non-linear Electroweak Chiral Lagrangian + the Inverse Amplitude Method (IAM).
- **Issue**: We need to plug the unitarized (IAM) scattering amplitudes (like $ww \to ww$ and $wz \to wz$) inside a bigger chain of hard scattering processes starting on partons, like: $pp \to W^+W^-jj$, $\boldsymbol{W^+W^- \to W^+W^-}$ **(IAM)**, $W^+ \to jj$, $W^- \to jj$
- **Issue**: Monte Carlo programs like MadGraph only understand Feynman Rules.
- **Solution**: an effective Proca Lagrangian is used to mimic the IAM amplitudes using the language of (effective) Feynman diagrams.
- This approach reminds those based on Form Factors, like Whizard or SHERPA. In the end, effective vertices on a BSM Monte-Carlo.
- However, this Effective Proca Lagrangian is meant to mimic the behaviour of unitarized amplitudes motivated on the analytical properties of the S-Matrix. Not a *simple form factor*.

Our EFT approach for Monte Carlo: Effective Proca Lagrangian

- We are using the Non-linear Electroweak Chiral Lagrangian + the Inverse Amplitude Method (IAM).
- **Issue**: We need to plug the unitarized (IAM) scattering amplitudes (like $ww \to ww$ and $wz \to wz$) inside a bigger chain of hard scattering processes starting on partons, like: $pp \to W^+W^-jj$, $\boldsymbol{W^+W^- \to W^+W^-}$ **(IAM)**, $W^+ \to jj$, $W^- \to jj$
- **Issue**: Monte Carlo programs like MadGraph only understand Feynman Rules.
- **Solution**: an effective Proca Lagrangian is used to mimic the IAM amplitudes using the language of (effective) Feynman diagrams.
- This approach reminds those based on Form Factors, like Whizard or SHERPA. In the end, effective vertices on a BSM Monte-Carlo.
- However, this Effective Proca Lagrangian is meant to mimic the behaviour of unitarized amplitudes motivated on the analytical properties of the S-Matrix. Not a *simple form factor*.

Our EFT approach for Monte Carlo: Effective Proca Lagrangian

- We are using the Non-linear Electroweak Chiral Lagrangian + the Inverse Amplitude Method (IAM).
- **Issue**: We need to plug the unitarized (IAM) scattering amplitudes (like $ww \to ww$ and $wz \to wz$) inside a bigger chain of hard scattering processes starting on partons, like: $pp \to W^+W^-jj$, $\boldsymbol{W^+W^- \to W^+W^-}$ **(IAM)**, $W^+ \to jj$, $W^- \to jj$
- **Issue**: Monte Carlo programs like MadGraph only understand Feynman Rules.
- **Solution**: an effective Proca Lagrangian is used to mimic the IAM amplitudes using the language of (effective) Feynman diagrams.
- This approach reminds those based on Form Factors, like Whizard or SHERPA. In the end, effective vertices on a BSM Monte-Carlo.
- However, this Effective Proca Lagrangian is meant to mimic the behaviour of unitarized amplitudes motivated on the analytical properties of the S-Matrix. Not a *simple form factor*.

Our EFT approach for Monte Carlo: Effective Proca Lagrangian

- We are using the Non-linear Electroweak Chiral Lagrangian + the Inverse Amplitude Method (IAM).
- **Issue**: We need to plug the unitarized (IAM) scattering amplitudes (like $ww \to ww$ and $wz \to wz$) inside a bigger chain of hard scattering processes starting on partons, like: $pp \to W^+W^-jj$, $\boldsymbol{W^+W^- \to W^+W^-}$ **(IAM)**, $W^+ \to jj$, $W^- \to jj$
- **Issue**: Monte Carlo programs like MadGraph only understand Feynman Rules.
- **Solution**: an effective Proca Lagrangian is used to mimic the IAM amplitudes using the language of (effective) Feynman diagrams.
- This approach reminds those based on Form Factors, like Whizard or SHERPA. In the end, effective vertices on a BSM Monte-Carlo.
- However, this Effective Proca Lagrangian is meant to mimic the behaviour of unitarized amplitudes motivated on the analytical properties of the S-Matrix. Not a *simple form factor*.

Our EFT approach for Monte Carlo: Effective Proca Lagrangian

- We are using the Non-linear Electroweak Chiral Lagrangian + the Inverse Amplitude Method (IAM).
- **Issue**: We need to plug the unitarized (IAM) scattering amplitudes (like $ww \to ww$ and $wz \to wz$) inside a bigger chain of hard scattering processes starting on partons, like: $pp \to W^+W^-jj$, $\boldsymbol{W^+W^- \to W^+W^-}$ **(IAM)**, $W^+ \to jj$, $W^- \to jj$
- **Issue**: Monte Carlo programs like MadGraph only understand Feynman Rules.
- **Solution**: an effective Proca Lagrangian is used to mimic the IAM amplitudes using the language of (effective) Feynman diagrams.
- This approach reminds those based on Form Factors, like Whizard or SHERPA. In the end, effective vertices on a BSM Monte-Carlo.
- However, this Effective Proca Lagrangian is meant to mimic the behaviour of unitarized amplitudes motivated on the analytical properties of the S-Matrix. Not a *simple form factor*.

Our EFT approach for Monte Carlo: Effective Proca Lagrangian

- We are using the Non-linear Electroweak Chiral Lagrangian + the Inverse Amplitude Method (IAM).
- **Issue**: We need to plug the unitarized (IAM) scattering amplitudes (like $ww \to ww$ and $wz \to wz$) inside a bigger chain of hard scattering processes starting on partons, like: $pp \to W^+W^-jj$, $\boldsymbol{W^+W^- \to W^+W^-}$ **(IAM)**, $W^+ \to jj$, $W^- \to jj$
- **Issue**: Monte Carlo programs like MadGraph only understand Feynman Rules.
- **Solution**: an effective Proca Lagrangian is used to mimic the IAM amplitudes using the language of (effective) Feynman diagrams.
- This approach reminds those based on Form Factors, like Whizard or SHERPA. In the end, effective vertices on a BSM Monte-Carlo.
- However, this Effective Proca Lagrangian is meant to mimic the behaviour of unitarized amplitudes motivated on the analytical properties of the S-Matrix. Not a *simple form factor*.

Diagrams for $WW \to WW$

EWChL

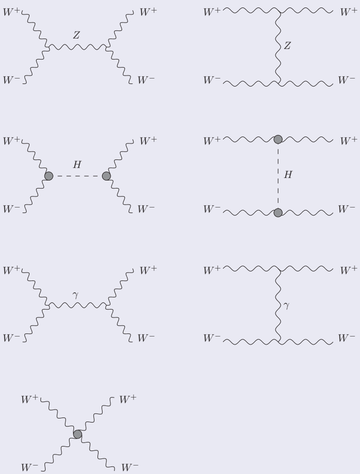

Eff. Proca

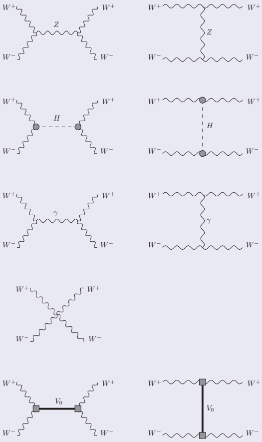

Channels: $W^+W^- \to W^+W^-$

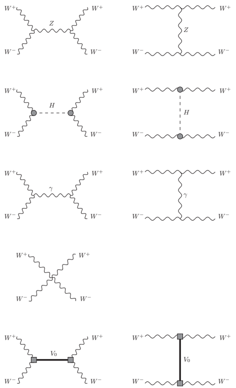

- We are extending our UFO for including $W^+W^- \to W^+W^-$.
- We expect to be able to deal with $WZ \to WZ$, $WW \to ZZ$, $ZZ \to WW$, $W^+W^- \to W^+W^-$, $W^\pm W^\pm \to W^\pm W^\pm$.
- On the longer term, we consider completing the EW model for including $ZZ \to ZZ$.
- The UFO model, actually, works.
- We have been granted 150kh of computer time of C2PAP for testing the new UFO.

Excellence Cluster Universe

Channels: $W^+W^- \to W^+W^-$

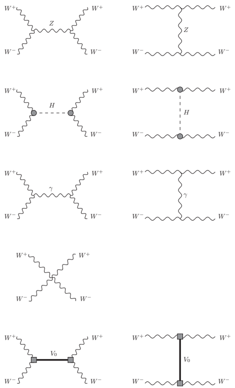

- We are extending our UFO for including $W^+W^- \to W^+W^-$.
- We expect to be able to deal with $WZ \to WZ$, $WW \to ZZ$, $ZZ \to WW$, $W^+W^- \to W^+W^-$, $W^\pm W^\pm \to W^\pm W^\pm$.
- On the longer term, we consider completing the EW model for including $ZZ \to ZZ$.
- The UFO model, actually, works.
- We have been granted 150kh of computer time of C2PAP for testing the new UFO.

Excellence Cluster Universe

Channels: $W^+W^- \to W^+W^-$

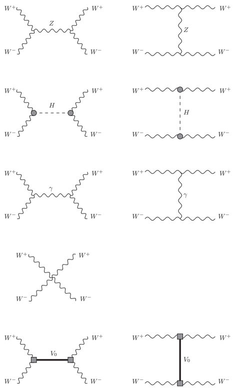

- We are extending our UFO for including $W^+W^- \to W^+W^-$.
- We expect to be able to deal with $WZ \to WZ$, $WW \to ZZ$, $ZZ \to WW$, $W^+W^- \to W^+W^-$, $W^\pm W^\pm \to W^\pm W^\pm$.
- On the longer term, we consider completing the EW model for including $ZZ \to ZZ$.
- The UFO model, actually, works.
- We have been granted 150kh of computer time of C2PAP for testing the new UFO.

Excellence Cluster Universe

Channels: $W^+W^- \to W^+W^-$

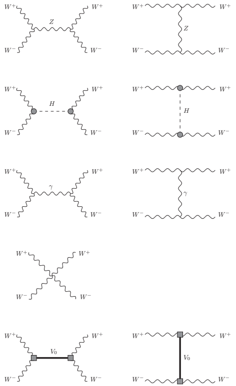

- We are extending our UFO for including $W^+W^- \to W^+W^-$.
- We expect to be able to deal with $WZ \to WZ$, $WW \to ZZ$, $ZZ \to WW$, $W^+W^- \to W^+W^-$, $W^\pm W^\pm \to W^\pm W^\pm$.
- On the longer term, we consider completing the EW model for including $ZZ \to ZZ$.
- The UFO model, actually, works.
- We have been granted 150kh of computer time of C2PAP for testing the new UFO.

Channels: $W^+W^- \to W^+W^-$

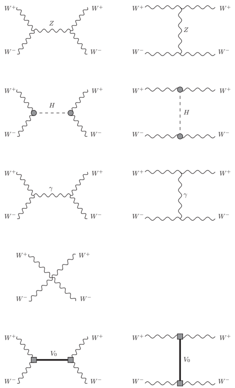

- We are extending our UFO for including $W^+W^- \to W^+W^-$.
- We expect to be able to deal with $WZ \to WZ$, $WW \to ZZ$, $ZZ \to WW$, $W^+W^- \to W^+W^-$, $W^\pm W^\pm \to W^\pm W^\pm$.
- On the longer term, we consider completing the EW model for including $ZZ \to ZZ$.
- The UFO model, actually, works.
- We have been granted 150kh of computer time of C2PAP for testing the new UFO.

Excellence Cluster Universe

Fully leptonic and fully hadronic channels, cuts

- On both analyses, we use standard **VBS cuts**. I.e., 2 jets (comming from parton scattering) with $2 < |\eta_{j_i}| < 5$, $p_T(j_i) > 20\,\mathrm{GeV}$ $(i = 1, 2)$, $M(j_1 j_2) > 500\,\mathrm{GeV}$, $\eta_{j_1} \cdot \eta_{j_2} < 0$.
- **Pythia 8** for hadronization + **DELPHES** (& FastJet) for jet reconstruction (anti-kT, $R = 0.5$) are used here.
- **Neutrino problem**: Missing Transverse Energy (MET) is an experimental observable at the LHC (hadron collider). BUT the component of the Missing Energy in the beamline direction is **LOST**.
- $\boldsymbol{W^+Z \to l^+\nu_l l^+ l^-}$, 1 single ν lost. Still, reconstructed transverse invariant mass $M^T_{lll\nu}$ shows a peak.
- $\boldsymbol{W^+W^- \to l^+l^-\nu_l\bar{\nu}_l}$, 2ν lost in fully leptonic channel. Reconstruction of a peak on $M^T_{ll\nu\nu}$ is not feasible.
- Our present research is on **fully hadronic channel** for W^+W^-, no MET. We assume boosted ($p_T > 200\,\mathrm{GeV}$) vector gauge bosons, that are recognized as a single fast jet on the detectors.

Fully leptonic and fully hadronic channels, cuts

- On both analyses, we use standard **VBS cuts**. I.e., 2 jets (comming from parton scattering) with $2 < |\eta_{j_i}| < 5$, $p_T(j_i) > 20\,\mathrm{GeV}$ $(i = 1, 2)$, $M(j_1 j_2) > 500\,\mathrm{GeV}$, $\eta_{j_1} \cdot \eta_{j_2} < 0$.
- **Pythia 8** for hadronization + **DELPHES** (& FastJet) for jet reconstruction (anti-kT, $R = 0.5$) are used here.
- **Neutrino problem**: Missing Transverse Energy (MET) is an experimental observable at the LHC (hadron collider). BUT the component of the Missing Energy in the beamline direction is **LOST**.
- $\boldsymbol{W^+ Z \to l^+ \nu_l l^+ l^-}$, 1 single ν lost. Still, reconstructed transverse invariant mass $M^T_{lll\nu}$ shows a peak.
- $\boldsymbol{W^+ W^- \to l^+ l^- \nu_l \bar{\nu}_l}$, 2ν lost in fully leptonic channel. Reconstruction of a peak on $M^T_{ll\nu\nu}$ is not feasible.
- Our present research is on **fully hadronic channel** for W^+W^-, no MET. We assume boosted ($p_T > 200\,\mathrm{GeV}$) vector gauge bosons, that are recognized as a single fast jet on the detectors.

Fully leptonic and fully hadronic channels, cuts

- On both analyses, we use standard **VBS cuts**. I.e., 2 jets (comming from parton scattering) with $2 < |\eta_{j_i}| < 5$, $p_T(j_i) > 20\,\mathrm{GeV}$ $(i = 1, 2)$, $M(j_1 j_2) > 500\,\mathrm{GeV}$, $\eta_{j_1} \cdot \eta_{j_2} < 0$.
- **Pythia 8** for hadronization + **DELPHES** (& FastJet) for jet reconstruction (anti-kT, $R = 0.5$) are used here.
- **Neutrino problem**: Missing Transverse Energy (MET) is an experimental observable at the LHC (hadron collider). BUT the component of the Missing Energy in the beamline direction is **LOST**.
- $\boldsymbol{W^+Z \to l^+\nu_l l^+ l^-}$, 1 single ν lost. Still, reconstructed transverse invariant mass $M^T_{lll\nu}$ shows a peak.
- $\boldsymbol{W^+W^- \to l^+l^-\nu_l\bar{\nu}_l}$, 2ν lost in fully leptonic channel. Reconstruction of a peak on $M^T_{ll\nu\nu}$ is not feasible.
- Our present research is on **fully hadronic channel** for W^+W^-, no MET. We assume boosted ($p_T > 200\,\mathrm{GeV}$) vector gauge bosons, that are recognized as a single fast jet on the detectors.

Fully leptonic and fully hadronic channels, cuts

- On both analyses, we use standard **VBS cuts**. I.e., 2 jets (comming from parton scattering) with $2 < |\eta_{j_i}| < 5$, $p_T(j_i) > 20\,\mathrm{GeV}$ ($i = 1, 2$), $M(j_1 j_2) > 500\,\mathrm{GeV}$, $\eta_{j_1} \cdot \eta_{j_2} < 0$.
- **Pythia 8** for hadronization + **DELPHES** (& FastJet) for jet reconstruction (anti-kT, $R = 0.5$) are used here.
- **Neutrino problem**: Missing Transverse Energy (MET) is an experimental observable at the LHC (hadron collider). BUT the component of the Missing Energy in the beamline direction is **LOST**.
- $\boldsymbol{W^+Z \to l^+\nu_l l^+ l^-}$, 1 single ν lost. Still, reconstructed transverse invariant mass $M^T_{lll\nu}$ shows a peak.
- $\boldsymbol{W^+W^- \to l^+l^-\nu_l\bar{\nu}_l}$, 2ν lost in fully leptonic channel. Reconstruction of a peak on $M^T_{ll\nu\nu}$ is not feasible.
- Our present research is on **fully hadronic channel** for W^+W^-, no MET. We assume boosted ($p_T > 200\,\mathrm{GeV}$) vector gauge bosons, that are recognized as a single fast jet on the detectors.

Fully leptonic and fully hadronic channels, cuts

- On both analyses, we use standard **VBS cuts**. I.e., 2 jets (comming from parton scattering) with $2 < |\eta_{j_i}| < 5$, $p_T(j_i) > 20\,\mathrm{GeV}$ $(i = 1, 2)$, $M(j_1 j_2) > 500\,\mathrm{GeV}$, $\eta_{j_1} \cdot \eta_{j_2} < 0$.
- **Pythia 8** for hadronization + **DELPHES** (& FastJet) for jet reconstruction (anti-kT, $R = 0.5$) are used here.
- **Neutrino problem**: Missing Transverse Energy (MET) is an experimental observable at the LHC (hadron collider). BUT the component of the Missing Energy in the beamline direction is **LOST**.
- $\boldsymbol{W^+ Z \to l^+ \nu_l l^+ l^-}$, 1 single ν lost. Still, reconstructed transverse invariant mass $M^T_{lll\nu}$ shows a peak.
- $\boldsymbol{W^+ W^- \to l^+ l^- \nu_l \bar{\nu}_l}$, 2ν lost in fully leptonic channel. Reconstruction of a peak on $M^T_{ll\nu\nu}$ is not feasible.
- Our present research is on **fully hadronic channel** for W^+W^-, no MET. We assume boosted ($p_T > 200\,\mathrm{GeV}$) vector gauge bosons, that are recognized as a single fast jet on the detectors.

Fully leptonic and fully hadronic channels, cuts

- On both analyses, we use standard **VBS cuts**. I.e., 2 jets (comming from parton scattering) with $2 < |\eta_{j_i}| < 5$, $p_T(j_i) > 20\,\mathrm{GeV}$ $(i = 1, 2)$, $M(j_1 j_2) > 500\,\mathrm{GeV}$, $\eta_{j_1} \cdot \eta_{j_2} < 0$.
- **Pythia 8** for hadronization + **DELPHES** (& FastJet) for jet reconstruction (anti-kT, $R = 0.5$) are used here.
- **Neutrino problem**: Missing Transverse Energy (MET) is an experimental observable at the LHC (hadron collider). BUT the component of the Missing Energy in the beamline direction is **LOST**.
- $\boldsymbol{W^+ Z \to l^+ \nu_l l^+ l^-}$, 1 single ν lost. Still, reconstructed transverse invariant mass $M^T_{lll\nu}$ shows a peak.
- $\boldsymbol{W^+ W^- \to l^+ l^- \nu_l \bar{\nu}_l}$, 2ν lost in fully leptonic channel. Reconstruction of a peak on $M^T_{ll\nu\nu}$ is not feasible.
- Our present research is on **fully hadronic channel** for $W^+ W^-$, no MET. We assume boosted ($p_T > 200\,\mathrm{GeV}$) vector gauge bosons, that are recognized as a single fast jet on the detectors.

Boosted vector gauge bosons

- Hypothesis: we have hadronic decays $W^+ \to jj$, $W^- \to jj$. But all the jets comming from a vector boson are reconstructed as a single fat jet (J) due to the original W being highly boosted, $p_T(J) > 200\,\mathrm{GeV}$.
- We reconstruct the original vector boson via de 4-momenta of the identified fat-jet. As a W-tagging, we use the invariant mass of the fat-jet (on a first approach). At the moment, $|\eta_J| < 2$, $p_T(J) > 200\,\mathrm{GeV}$ and $R = 0.8$.
- We are considering τ_{21}, $M(J)$ for W–tagging. See, for instance:
  - JHEP 12 (2014) 017, CMS-JME-13-006, CERN-PH-EP-2014-241
  - CERN-EP-2018-192, arXiv:1808.07858 [hep-ex]
  - See next slide: `https://indico.cern.ch/event/576047/contributions/2356506/attachments/1380679/2098953/161130CMS_WZTagging.pdf`

Boosted vector gauge bosons

- Hypothesis: we have hadronic decays $W^+ \to jj$, $W^- \to jj$. But all the jets comming from a vector boson are reconstructed as a single fat jet (J) due to the original W being highly boosted, $p_T(J) > 200\,\mathrm{GeV}$.
- We reconstruct the original vector boson via de 4-momenta of the identified fat-jet. As a W-tagging, we use the invariant mass of the fat-jet (on a first approach). At the moment, $|\eta_J| < 2$, $p_T(J) > 200\,\mathrm{GeV}$ and $R = 0.8$.
- We are considering τ_{21}, $M(J)$ for W–tagging. See, for instance:
  - JHEP 12 (2014) 017, CMS-JME-13-006, CERN-PH-EP-2014-241
  - CERN-EP-2018-192, arXiv:1808.07858 [hep-ex]
  - See next slide: `https://indico.cern.ch/event/576047/contributions/2356506/attachments/1380679/2098953/161130CMS_WZTagging.pdf`

Boosted vector gauge bosons

- Hypothesis: we have hadronic decays $W^+ \to jj$, $W^- \to jj$. But all the jets comming from a vector boson are reconstructed as a single fat jet (J) due to the original W being highly boosted, $p_T(J) > 200\,\mathrm{GeV}$.
- We reconstruct the original vector boson via de 4-momenta of the identified fat-jet. As a W-tagging, we use the invariant mass of the fat-jet (on a first approach). At the moment, $|\eta_J| < 2$, $p_T(J) > 200\,\mathrm{GeV}$ and $R = 0.8$.
- We are considering τ_{21}, $M(J)$ for W–tagging. See, for instance:
  - JHEP 12 (2014) 017, CMS-JME-13-006, CERN-PH-EP-2014-241
  - CERN-EP-2018-192, arXiv:1808.07858 [hep-ex]
  - See next slide: `https://indico.cern.ch/event/576047/contributions/2356506/attachments/1380679/2098953/161130CMS_WZTagging.pdf`

Boosted vector gauge bosons

- Hypothesis: we have hadronic decays $W^+ \to jj$, $W^- \to jj$. But all the jets comming from a vector boson are reconstructed as a single fat jet (J) due to the original W being highly boosted, $p_T(J) > 200\,\mathrm{GeV}$.
- We reconstruct the original vector boson via de 4-momenta of the identified fat-jet. As a W-tagging, we use the invariant mass of the fat-jet (on a first approach). At the moment, $|\eta_J| < 2$, $p_T(J) > 200\,\mathrm{GeV}$ and $R = 0.8$.
- We are considering τ_{21}, $M(J)$ for W–tagging. See, for instance:
  - JHEP 12 (2014) 017, CMS-JME-13-006, CERN-PH-EP-2014-241
  - CERN-EP-2018-192, arXiv:1808.07858 [hep-ex]
  - See next slide: `https://indico.cern.ch/event/576047/contributions/2356506/attachments/1380679/2098953/161130CMS_WZTagging.pdf`

Boosted vector gauge bosons

- Hypothesis: we have hadronic decays $W^+ \to jj$, $W^- \to jj$. But all the jets comming from a vector boson are reconstructed as a single fat jet (J) due to the original W being highly boosted, $p_T(J) > 200\,\mathrm{GeV}$.
- We reconstruct the original vector boson via de 4-momenta of the identified fat-jet. As a W-tagging, we use the invariant mass of the fat-jet (on a first approach). At the moment, $|\eta_J| < 2$, $p_T(J) > 200\,\mathrm{GeV}$ and $R = 0.8$.
- We are considering τ_{21}, $M(J)$ for W–tagging. See, for instance:
  - JHEP 12 (2014) 017, CMS-JME-13-006, CERN-PH-EP-2014-241
  - CERN-EP-2018-192, arXiv:1808.07858 [hep-ex]
  - See next slide: `https://indico.cern.ch/event/576047/contributions/2356506/attachments/1380679/2098953/161130CMS_WZTagging.pdf`

Boosted vector gauge bosons

- Hypothesis: we have hadronic decays $W^+ \to jj$, $W^- \to jj$. But all the jets comming from a vector boson are reconstructed as a single fat jet (J) due to the original W being highly boosted, $p_T(J) > 200\,\mathrm{GeV}$.
- We reconstruct the original vector boson via de 4-momenta of the identified fat-jet. As a W-tagging, we use the invariant mass of the fat-jet (on a first approach). At the moment, $|\eta_J| < 2$, $p_T(J) > 200\,\mathrm{GeV}$ and $R = 0.8$.
- We are considering τ_{21}, $M(J)$ for W–tagging. See, for instance:
    - JHEP 12 (2014) 017, CMS-JME-13-006, CERN-PH-EP-2014-241
    - CERN-EP-2018-192, arXiv:1808.07858 [hep-ex]
    - See next slide: `https://indico.cern.ch/event/576047/contributions/2356506/attachments/1380679/2098953/161130CMS_WZTagging.pdf`

Boosted vector gauge bosons: [Cristina Mantilla Suarez (Johns Hopkins)]

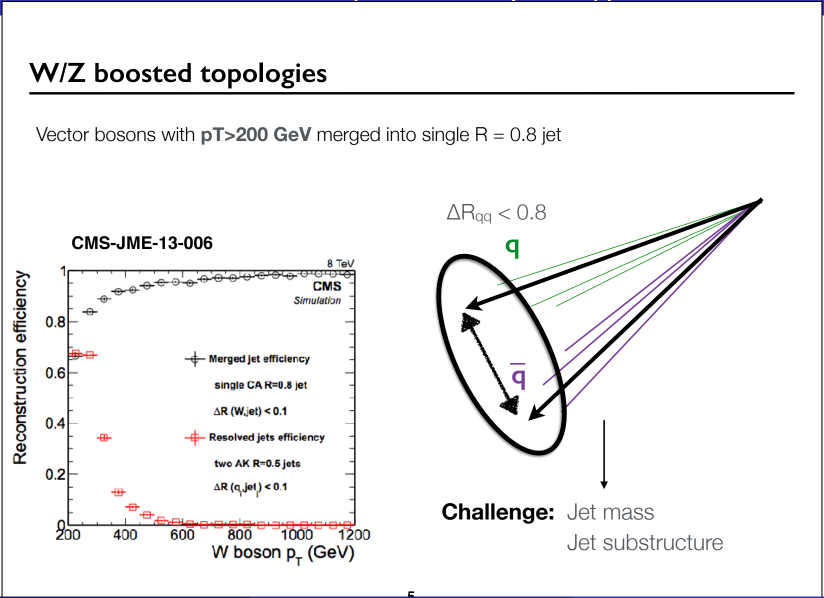

W/Z boosted topologies

Vector bosons with **pT>200 GeV** merged into single R = 0.8 jet

CMS-JME-13-006

Challenge: Jet mass
Jet substructure

Considered background: hadronic channel, W^+W^-

- **Signal**: $pp \to jjW^+W^-$, $W^+ \to jj$, $W^- \to jj$. Note that we only identify fat jets, $W^\pm \to J$.
- Pure **SM-EW Background**, amplitude of order $\mathcal{O}(\alpha_{\rm em}^2)$. Followed by hadronic decay of WW.
- Mixed **SM-EWQCD Background**, amplitude of order $\mathcal{O}(\alpha_{\rm em}\alpha_{\rm s})$. Followed by hadronic decay of WW.
- **QCD Background**: all LO-QCD $pp \to 4j$ processes, that mimic a signal with 2 jets + 2 fat-jet ($M(J) \sim M_W$). This background is both high and very difficult to remove. W-tagging techniques from our experimentalist colleagues (previous slides) are helpful for dealing with this background.
- $t\bar{t}$ **Background**: processes like $pp \to t\bar{t} \to b\bar{b}W^+W^-$, where the pair $b\bar{b}$ mimics the 2 light jet signal comming from a VBS event. This background, in practise, is greatly removed by b–tagging and usual VBS cuts. However, it is extremely challenging to simulate. Work in progress.

Considered background: hadronic channel, W^+W^-

- **Signal**: $pp \to jjW^+W^-$, $W^+ \to jj$, $W^- \to jj$. Note that we only identify fat jets, $W^\pm \to J$.
- Pure **SM-EW Background**, amplitude of order $\mathcal{O}(\alpha_{\rm em}^2)$. Followed by hadronic decay of WW.
- Mixed **SM-EWQCD Background**, amplitude of order $\mathcal{O}(\alpha_{\rm em}\alpha_{\rm s})$. Followed by hadronic decay of WW.
- **QCD Background**: all LO-QCD $pp \to 4j$ processes, that mimic a signal with 2 jets + 2 fat-jet ($M(J) \sim M_W$). This background is both high and very difficult to remove. W-tagging techniques from our experimentalist colleagues (previous slides) are helpful for dealing with this background.
- **$t\bar{t}$ Background**: processes like $pp \to t\bar{t} \to b\bar{b}W^+W^-$, where the pair $b\bar{b}$ mimics the 2 light jet signal comming from a VBS event. This background, in practise, is greatly removed by b–tagging and usual VBS cuts. However, it is extremely challenging to simulate. Work in progress.

Considered background: hadronic channel, W^+W^-

- **Signal**: $pp \to jjW^+W^-$, $W^+ \to jj$, $W^- \to jj$. Note that we only identify fat jets, $W^\pm \to J$.
- Pure **SM-EW Background**, amplitude of order $\mathcal{O}(\alpha_{\rm em}^2)$. Followed by hadronic decay of WW.
- Mixed **SM-EWQCD Background**, amplitude of order $\mathcal{O}(\alpha_{\rm em}\alpha_{\rm s})$. Followed by hadronic decay of WW.
- **QCD Background**: all LO-QCD $pp \to 4j$ processes, that mimic a signal with 2 jets + 2 fat-jet ($M(J) \sim M_W$). This background is both high and very difficult to remove. W-tagging techniques from our experimentalist colleagues (previous slides) are helpful for dealing with this background.
- **$t\bar{t}$ Background**: processes like $pp \to t\bar{t} \to b\bar{b}W^+W^-$, where the pair $b\bar{b}$ mimics the 2 light jet signal comming from a VBS event. This background, in practise, is greatly removed by b–tagging and usual VBS cuts. However, it is extremely challenging to simulate. Work in progress.

Considered background: hadronic channel, W^+W^-

- **Signal**: $pp \to jjW^+W^-$, $W^+ \to jj$, $W^- \to jj$. Note that we only identify fat jets, $W^\pm \to J$.
- Pure **SM-EW Background**, amplitude of order $\mathcal{O}(\alpha_{\rm em}^2)$. Followed by hadronic decay of WW.
- Mixed **SM-EWQCD Background**, amplitude of order $\mathcal{O}(\alpha_{\rm em}\alpha_{\rm s})$. Followed by hadronic decay of WW.
- **QCD Background**: all LO-QCD $pp \to 4j$ processes, that mimic a signal with 2 jets + 2 fat-jet ($M(J) \sim M_W$). This background is both high and very difficult to remove. W-tagging techniques from our experimentalist colleagues (previous slides) are helpful for dealing with this background.
- **$t\bar{t}$ Background**: processes like $pp \to t\bar{t} \to b\bar{b}W^+W^-$, where the pair $b\bar{b}$ mimics the 2 light jet signal comming from a VBS event. This background, in practise, is greatly removed by b–tagging and usual VBS cuts. However, it is extremely challenging to simulate. Work in progress.

Considered background: hadronic channel, W^+W^-

- **Signal**: $pp \to jjW^+W^-$, $W^+ \to jj$, $W^- \to jj$. Note that we only identify fat jets, $W^\pm \to J$.
- Pure **SM-EW Background**, amplitude of order $\mathcal{O}(\alpha_{\rm em}^2)$. Followed by hadronic decay of WW.
- Mixed **SM-EWQCD Background**, amplitude of order $\mathcal{O}(\alpha_{\rm em}\alpha_{\rm s})$. Followed by hadronic decay of WW.
- **QCD Background**: all LO-QCD $pp \to 4j$ processes, that mimic a signal with 2 jets + 2 fat-jet ($M(J) \sim M_W$). This background is both high and very difficult to remove. W-tagging techniques from our experimentalist colleagues (previous slides) are helpful for dealing with this background.
- **$t\bar{t}$ Background**: processes like $pp \to t\bar{t} \to b\bar{b}W^+W^-$, where the pair $b\bar{b}$ mimics the 2 light jet signal comming from a VBS event. This background, in practise, is greatly removed by b–tagging and usual VBS cuts. However, it is extremely challenging to simulate. Work in progress.

WW hadronic final state, PRELIMINAR: BP1

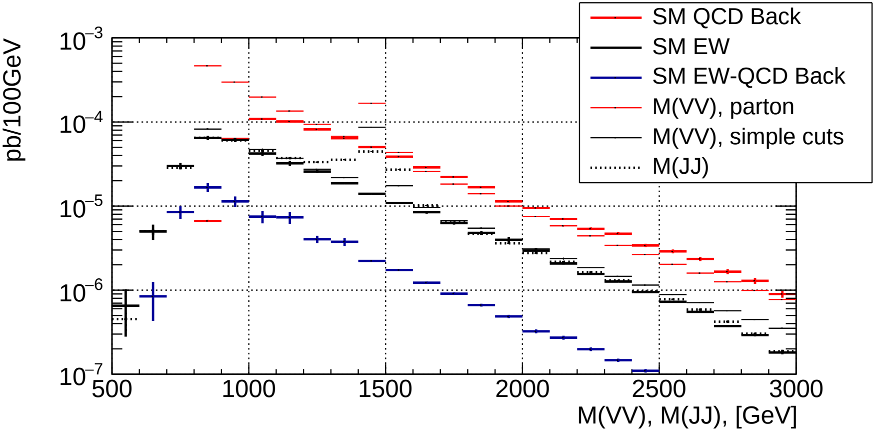

2 fat-jets ($p_T > 200\,\mathrm{GeV}$), anti-kT ($R = 0.8$), up to 4 extra thin-jets.
$M(VV)$, MadGraph 5, before Pythia8+DELPHES.
Note: SM QCD, factor 10^{-2}!!

WW hadronic final state, PRELIMINAR: BP*i*

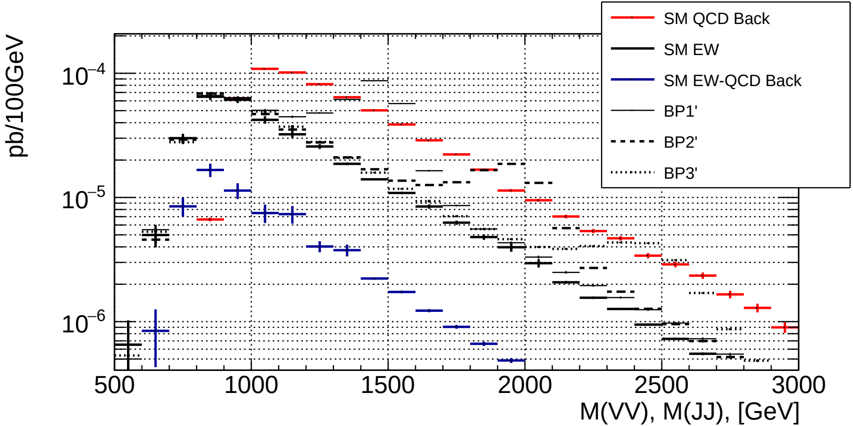

2 fat-jets ($p_T > 200\,\mathrm{GeV}$), anti-kT ($R = 0.8$), up to 4 extra thin-jets.
$M(VV)$, MadGraph 5, before Pythia8+DELPHES.
Note: SM QCD, factor 10^{-2}!!

WW hadronic final state, PRELIMINAR: BP*i*'

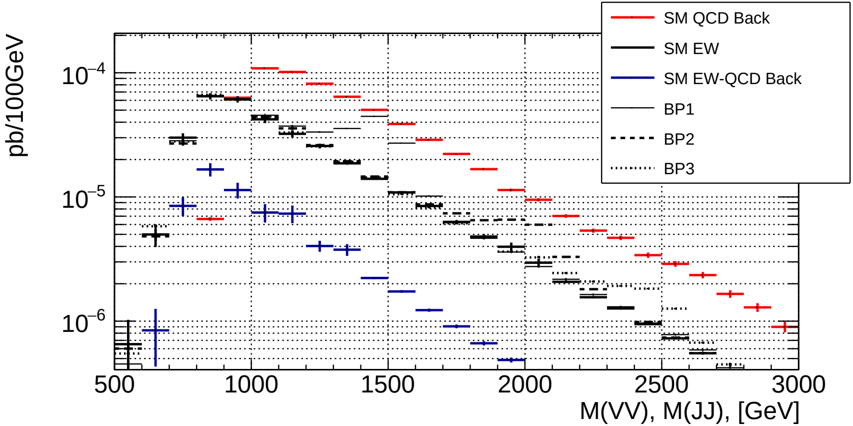

2 fat-jets ($p_T > 200\,\mathrm{GeV}$), anti-kT ($R = 0.8$), up to 4 extra thin-jets.
$M(VV)$, MadGraph 5, before Pythia8+DELPHES.
Note: SM QCD, factor 10^{-2}!!

WW hadronic final state, PRELIMINAR: τ_{21}

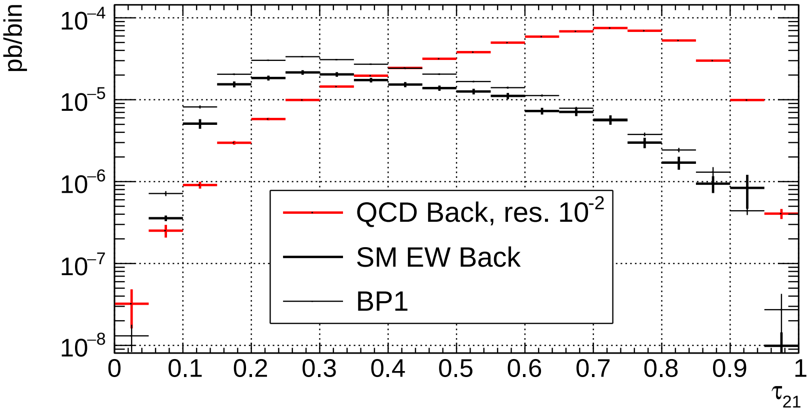

2 fat-jets ($p_T > 200\,\mathrm{GeV}$), anti-kT ($R = 0.8$), up to 4 extra thin-jets.
$M(VV)$, MadGraph 5, before Pythia8+DELPHES.
Note: SM QCD, factor 10^{-2}!!

Expected events for WW (fully hadronic), preliminar

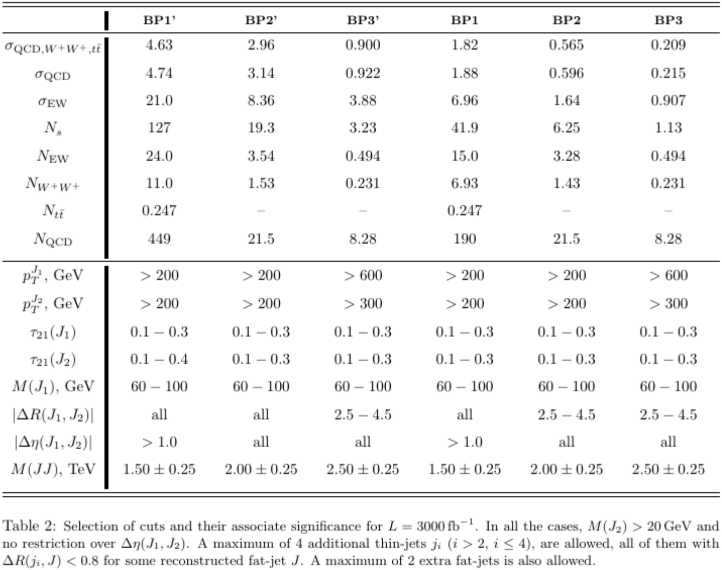

	BP1'	**BP2'**	**BP3'**	**BP1**	**BP2**	**BP3**
$\sigma_{\text{QCD},W^+W^+,t\bar{t}}$	4.63	2.96	0.900	1.82	0.565	0.209
σ_{QCD}	4.74	3.14	0.922	1.88	0.596	0.215
σ_{EW}	21.0	8.36	3.88	6.96	1.64	0.907
N_s	127	19.3	3.23	41.9	6.25	1.13
N_{EW}	24.0	3.54	0.494	15.0	3.28	0.494
$N_{W^+W^+}$	11.0	1.53	0.231	6.93	1.43	0.231
$N_{t\bar{t}}$	0.247	–	–	0.247	–	–
N_{QCD}	449	21.5	8.28	190	21.5	8.28
$p_T^{J_1}$, GeV	> 200	> 200	> 600	> 200	> 200	> 600
$p_T^{J_2}$, GeV	> 200	> 200	> 300	> 200	> 200	> 300
$\tau_{21}(J_1)$	$0.1 - 0.3$	$0.1 - 0.3$	$0.1 - 0.3$	$0.1 - 0.3$	$0.1 - 0.3$	$0.1 - 0.3$
$\tau_{21}(J_2)$	$0.1 - 0.4$	$0.1 - 0.3$	$0.1 - 0.3$	$0.1 - 0.3$	$0.1 - 0.3$	$0.1 - 0.3$
$M(J_1)$, GeV	$60 - 100$	$60 - 100$	$60 - 100$	$60 - 100$	$60 - 100$	$60 - 100$
$\|\Delta R(J_1, J_2)\|$	all	all	$2.5 - 4.5$	all	$2.5 - 4.5$	$2.5 - 4.5$
$\|\Delta\eta(J_1, J_2)\|$	> 1.0	all	all	> 1.0	all	all
$M(JJ)$, TeV	1.50 ± 0.25	2.00 ± 0.25	2.50 ± 0.25	1.50 ± 0.25	2.00 ± 0.25	2.50 ± 0.25

Table 2: Selection of cuts and their associate significance for $L = 3000\,\text{fb}^{-1}$. In all the cases, $M(J_2) > 20\,\text{GeV}$ and no restriction over $\Delta\eta(J_1, J_2)$. A maximum of 4 additional thin-jets j_i ($i > 2$, $i \leq 4$), are allowed, all of them with $\Delta R(j_i, J) < 0.8$ for some reconstructed fat-jet J. A maximum of 2 extra fat-jets is also allowed.

Diagrams for $WZ \to WZ$

EWChL

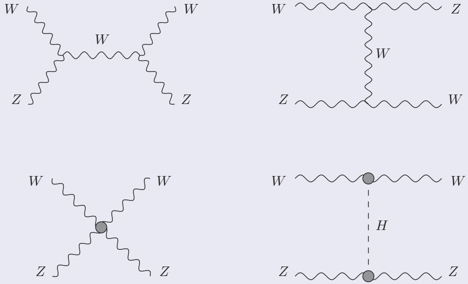

Eff. Proca

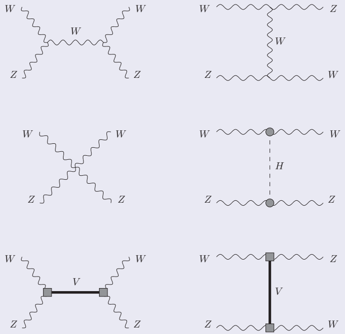

Legend

Grey circles: BSM Chiral parameters, a, b, a_4, a_5.
Grey boxes: effective Proca couplings.

Channels: $WZ \to WZ$

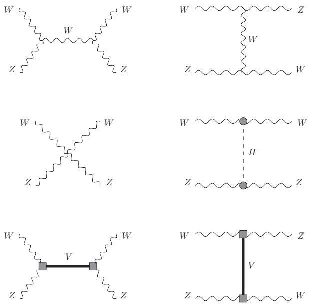

- We are using MadGraph v5 capability of integrating Fortran code inside UFO.
- We encode the Proca processes (those involving the resonace V) as effective vertices inside the UFO.
- The parameters of the Proca Lagrangian are adjusted to the IAM results [dynamic M_V, Γ_V, $g_V(M_V^2)$] via a custom piece of software.
- Currently, $W^+Z \to W^+Z$ tested.
- Leptonic channel studied: $pp \to w^+zjj$, $w^+ \to l^+\nu$, $z \to l^+l^-$

Channels: $WZ \to WZ$

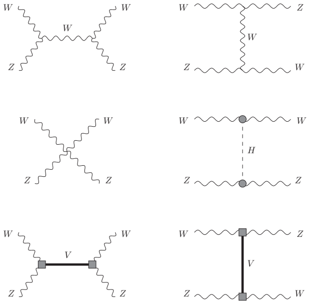

- We are using MadGraph v5 capability of integrating Fortran code inside UFO.
- We encode the Proca processes (those involving the resonance V) as effective vertices inside the UFO.
- The parameters of the Proca Lagrangian are adjusted to the IAM results [dynamic M_V, Γ_V, $g_V(M_V^2)$] via a custom piece of software.
- Currently, $W^+Z \to W^+Z$ tested.
- Leptonic channel studied: $pp \to w^+zjj$, $w^+ \to l^+\nu$, $z \to l^+l^-$

Channels: $WZ \to WZ$

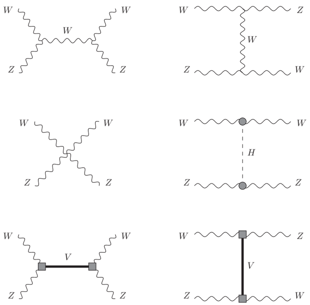

- We are using MadGraph v5 capability of integrating Fortran code inside UFO.
- We encode the Proca processes (those involving the resonace V) as effective vertices inside the UFO.
- The parameters of the Proca Lagrangian are adjusted to the IAM results [dynamic M_V, Γ_V, $g_V(M_V^2)$] via a custom piece of software.
- Currently, $W^+Z \to W^+Z$ tested.
- Leptonic channel studied: $pp \to w^+zjj$, $w^+ \to l^+\nu$, $z \to l^+l^-$

Channels: $WZ \to WZ$

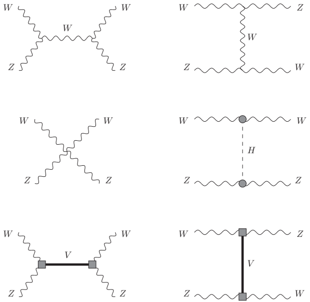

- We are using MadGraph v5 capability of integrating Fortran code inside UFO.
- We encode the Proca processes (those involving the resonace V) as effective vertices inside the UFO.
- The parameters of the Proca Lagrangian are adjusted to the IAM results [dynamic M_V, Γ_V, $g_V(M_V^2)$] via a custom piece of software.
- Currently, $W^+Z \to W^+Z$ tested.
- Leptonic channel studied: $pp \to w^+zjj$, $w^+ \to l^+\nu$, $z \to l^+l^-$

Channels: $WZ \to WZ$

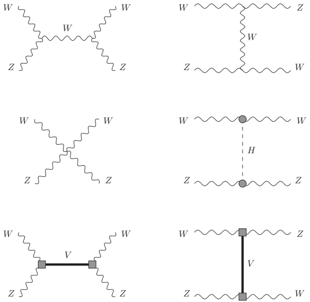

- We are using MadGraph v5 capability of integrating Fortran code inside UFO.
- We encode the Proca processes (those involving the resonace V) as effective vertices inside the UFO.
- The parameters of the Proca Lagrangian are adjusted to the IAM results [dynamic M_V, Γ_V, $g_V(M_V^2)$] via a custom piece of software.
- Currently, $W^+Z \to W^+Z$ tested.
- Leptonic channel studied: $pp \to w^+zjj$, $w^+ \to l^+\nu$, $z \to l^+l^-$

Considered background: leptonic channel, W^+Z

- **Signal**: $pp \to jjW^+Z$, $W^+ \to l^+\nu$, $Z \to l^+l^-$
- Pure **SM-EW Background**, amplitude of order $\mathcal{O}(\alpha_{\rm em}^2)$. Followed by leptonic decay of W^+Z.
- Mixed **SM-EWQCD Background**, amplitude of order $\mathcal{O}(\alpha_{\rm em}\alpha_{\rm s})$. Followed by leptonic decay of W^+Z.

Considered background: leptonic channel, W^+Z

- **Signal**: $pp \to jjW^+Z$, $W^+ \to l^+\nu$, $Z \to l^+l^-$
- Pure **SM-EW Background**, amplitude of order $\mathcal{O}(\alpha_{\rm em}^2)$. Followed by leptonic decay of W^+Z.
- Mixed **SM-EWQCD Background**, amplitude of order $\mathcal{O}(\alpha_{\rm em}\alpha_{\rm s})$. Followed by leptonic decay of W^+Z.

Considered background: leptonic channel, W^+Z

- **Signal**: $pp \to jjW^+Z$, $W^+ \to l^+\nu$, $Z \to l^+l^-$
- Pure **SM-EW Background**, amplitude of order $\mathcal{O}(\alpha_{\rm em}^2)$. Followed by leptonic decay of W^+Z.
- Mixed **SM-EWQCD Background**, amplitude of order $\mathcal{O}(\alpha_{\rm em}\alpha_{\rm s})$. Followed by leptonic decay of W^+Z.

Expected events for WZ (leptonic)

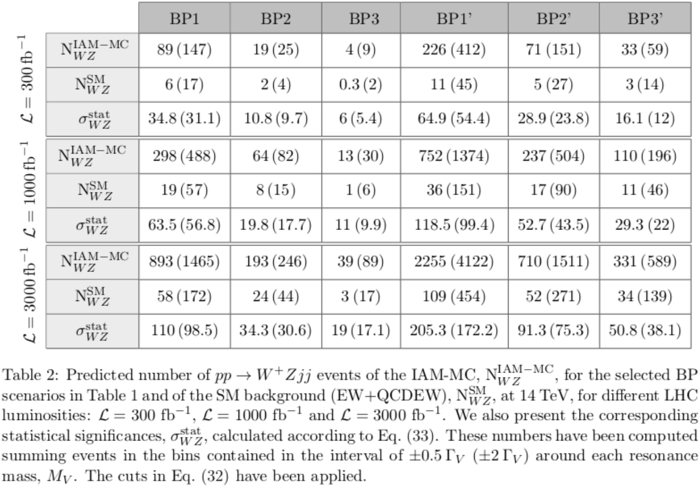

		BP1	BP2	BP3	BP1'	BP2'	BP3'
$\mathcal{L} = 300\ \text{fb}^{-1}$	$\text{N}_{WZ}^{\text{IAM-MC}}$	89 (147)	19 (25)	4 (9)	226 (412)	71 (151)	33 (59)
	$\text{N}_{WZ}^{\text{SM}}$	6 (17)	2 (4)	0.3 (2)	11 (45)	5 (27)	3 (14)
	$\sigma_{WZ}^{\text{stat}}$	34.8 (31.1)	10.8 (9.7)	6 (5.4)	64.9 (54.4)	28.9 (23.8)	16.1 (12)
$\mathcal{L} = 1000\ \text{fb}^{-1}$	$\text{N}_{WZ}^{\text{IAM-MC}}$	298 (488)	64 (82)	13 (30)	752 (1374)	237 (504)	110 (196)
	$\text{N}_{WZ}^{\text{SM}}$	19 (57)	8 (15)	1 (6)	36 (151)	17 (90)	11 (46)
	$\sigma_{WZ}^{\text{stat}}$	63.5 (56.8)	19.8 (17.7)	11 (9.9)	118.5 (99.4)	52.7 (43.5)	29.3 (22)
$\mathcal{L} = 3000\ \text{fb}^{-1}$	$\text{N}_{WZ}^{\text{IAM-MC}}$	893 (1465)	193 (246)	39 (89)	2255 (4122)	710 (1511)	331 (589)
	$\text{N}_{WZ}^{\text{SM}}$	58 (172)	24 (44)	3 (17)	109 (454)	52 (271)	34 (139)
	$\sigma_{WZ}^{\text{stat}}$	110 (98.5)	34.3 (30.6)	19 (17.1)	205.3 (172.2)	91.3 (75.3)	50.8 (38.1)

Table 2: Predicted number of $pp \to W^+Zjj$ events of the IAM-MC, $\text{N}_{WZ}^{\text{IAM-MC}}$, for the selected BP scenarios in Table 1 and of the SM background (EW+QCDEW), $\text{N}_{WZ}^{\text{SM}}$, at 14 TeV, for different LHC luminosities: $\mathcal{L} = 300\ \text{fb}^{-1}$, $\mathcal{L} = 1000\ \text{fb}^{-1}$ and $\mathcal{L} = 3000\ \text{fb}^{-1}$. We also present the corresponding statistical significances, $\sigma_{WZ}^{\text{stat}}$, calculated according to Eq. (33). These numbers have been computed summing events in the bins contained in the interval of $\pm 0.5\,\Gamma_V$ $(\pm 2\,\Gamma_V)$ around each resonance mass, M_V. The cuts in Eq. (32) have been applied.

RESULTS: *WZ* in final state

JHEP1711, 098

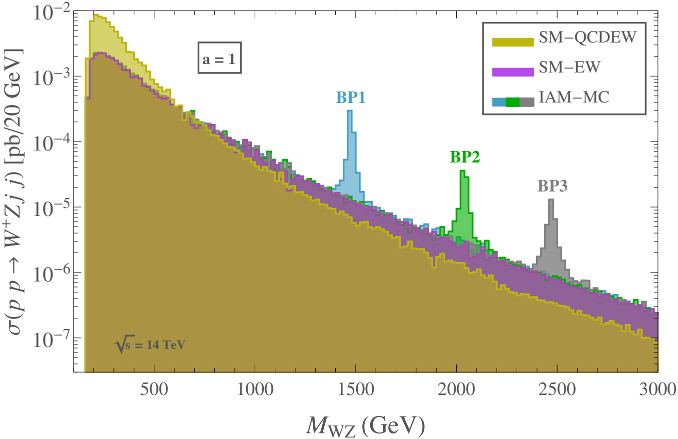

$a = 1$; $a_4 \cdot 10^4 = 3.5$ (BP1), 1 (BP2), 0.5 (BP3);

$-a_5 \cdot 10^4 = 3$ (BP1), 1 (BP2), 0.5 (BP3).

RESULTS: *WZ* in leptonic final state

JHEP1711, 098

Transverse Mass $M^T_{lll\nu}$ used here: ν longitudinal momentum lost!!

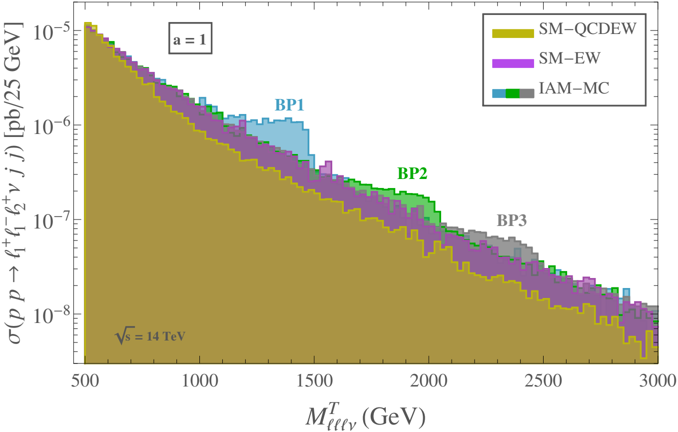

$a = 1$; $a_4 \cdot 10^4 = 3.5$ (BP1), 1 (BP2), 0.5 (BP3);

$-a_5 \cdot 10^4 = 3$ (BP1), 1 (BP2), 0.5 (BP3).

WW hadronic final state, PRELIMINAR: BP1

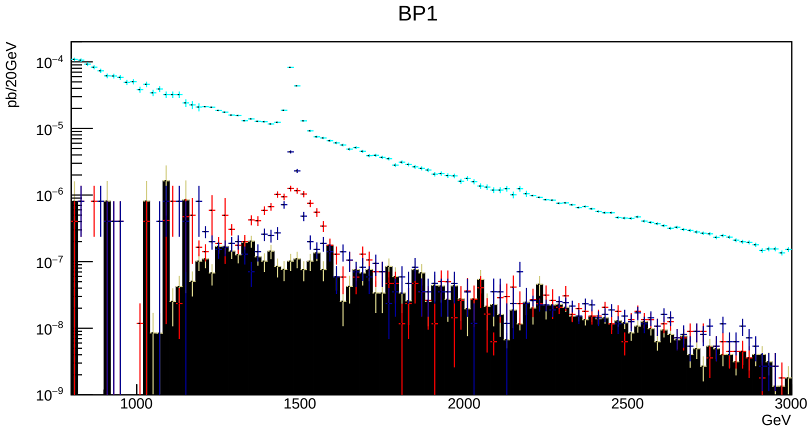

parton lev. $M(WW)$ NO PY8/DELPH. (cyan); $M(WW)$, DELPHES cuts (blue)

fat jet reconstr. $M(JJ)$ (red); SM-EW backgr. (black)

$70\,\mathrm{GeV} < M(J) < 90\,\mathrm{GeV}$; BP1: $M(V) = 1476\,\mathrm{GeV}$, $\Gamma(V) = 14\,\mathrm{GeV}$.

WW hadronic final state, PRELIMINAR: BP2

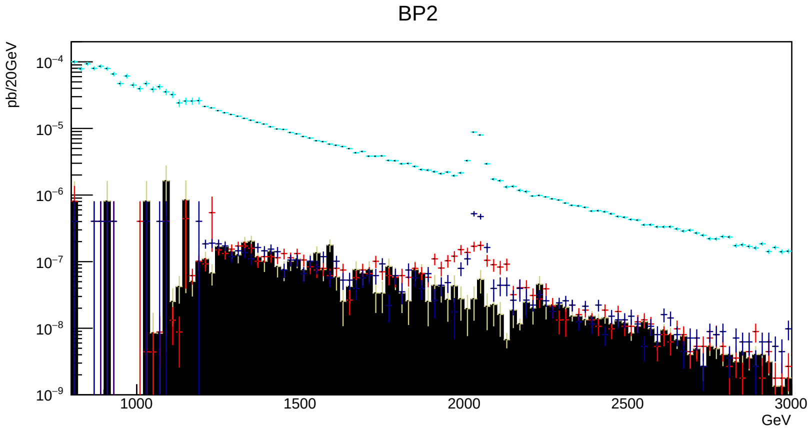

parton lev. $M(WW)$ NO PY8/DELPH. (cyan); $M(WW)$, DELPHES cuts (blue)

fat jet reconstr. $M(JJ)$ (red); SM-EW backgr. (black)

$70\,\mathrm{GeV} < M(J) < 90\,\mathrm{GeV}$; BP2: $M(V) = 2039\,\mathrm{GeV}$, $\Gamma(V) = 21\,\mathrm{GeV}$.

WW hadronic final state, PRELIMINAR: BP3

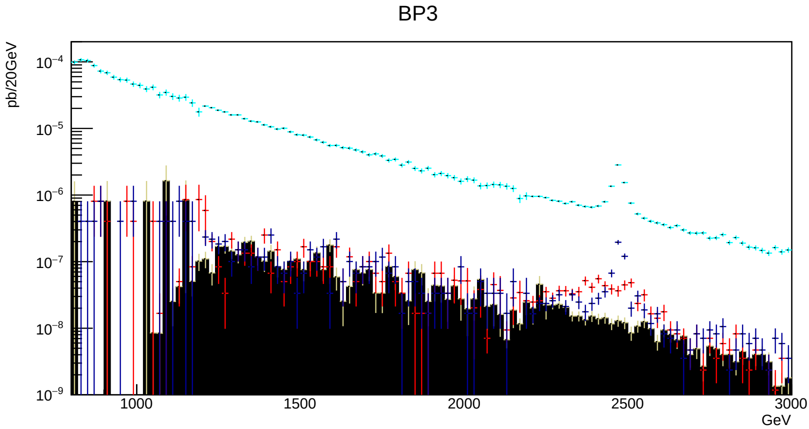

parton lev. $M(WW)$ NO PY8/DELPH. (cyan); $M(WW)$, DELPHES cuts (blue)

fat jet reconstr. $M(JJ)$ (red); SM-EW backgr. (black)

$70\,\mathrm{GeV} < M(J) < 90\,\mathrm{GeV}$; BP3: $M(V) = 2472\,\mathrm{GeV}$, $\Gamma(V) = 27\,\mathrm{GeV}$.

WW hadronic final state: QCD background vs BP3

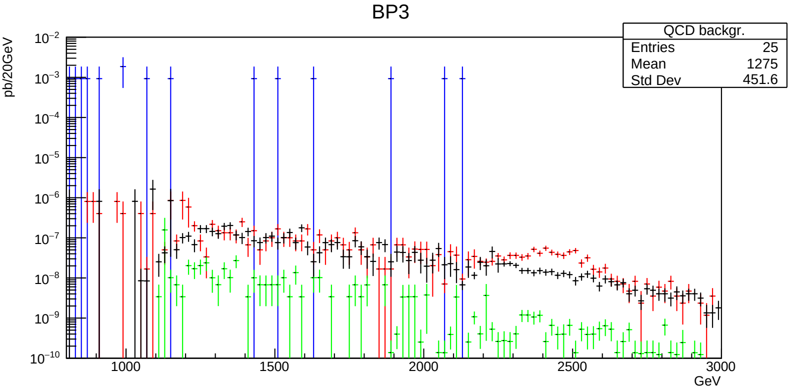

BP3 signal (red); SM-EW backgr. (black)

SM-QCDEW backgr. (green); $M(JJ)$, QCD background (blue)

$70\,\mathrm{GeV} < M(J) < 90\,\mathrm{GeV}$; BP3: $M(V) = 2472\,\mathrm{GeV}$, $\Gamma(V) = 27\,\mathrm{GeV}$.

WW hadronic final state: QCD background vs BP3

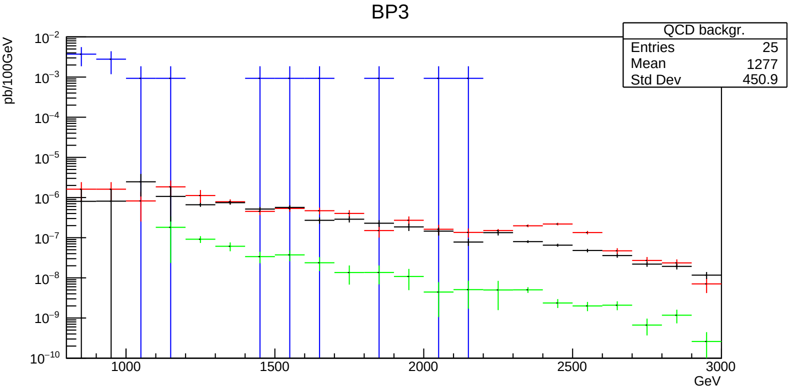

BP3 signal (red); SM-EW backgr. (black)

SM-QCDEW backgr. (green); $M(JJ)$, QCD background (blue)

$70\,\mathrm{GeV} < M(J) < 90\,\mathrm{GeV}$; BP3: $M(V) = 2472\,\mathrm{GeV}$, $\Gamma(V) = 27\,\mathrm{GeV}$.

WW hadronic final state: QCD background vs BP3

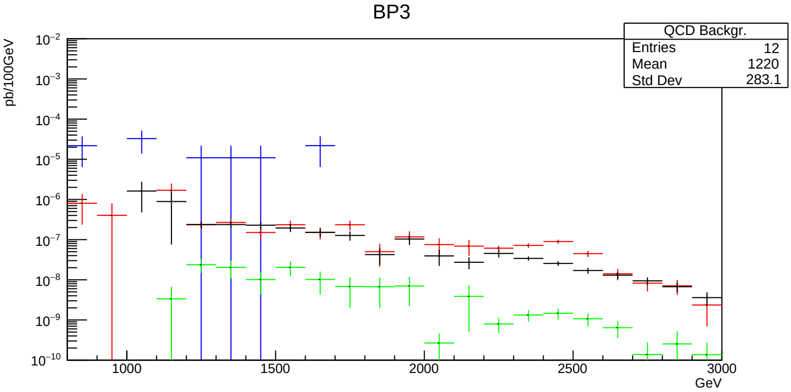

BP3 signal (red); SM-EW backgr. (black)

SM-QCDEW backgr. (green); $M(JJ)$, QCD background (blue)

$75\,\mathrm{GeV} < M(J) < 85\,\mathrm{GeV}$; BP3: $M(V) = 2472\,\mathrm{GeV}$, $\Gamma(V) = 27\,\mathrm{GeV}$.

WW hadronic final state: QCD background vs BP3

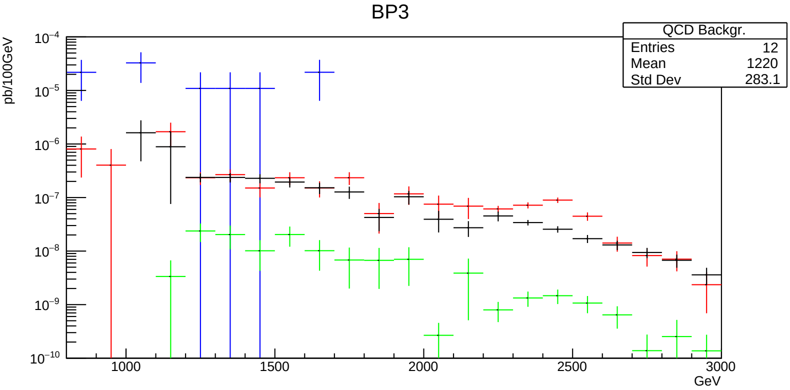

BP3 signal (red); SM-EW backgr. (black)

SM-QCDEW backgr. (green); $M(JJ)$, QCD background (blue)

$75\,\mathrm{GeV} < M(J) < 85\,\mathrm{GeV}$; BP3: $M(V) = 2472\,\mathrm{GeV}$, $\Gamma(V) = 27\,\mathrm{GeV}$.

Experimental constraints

JHEP1711, 098

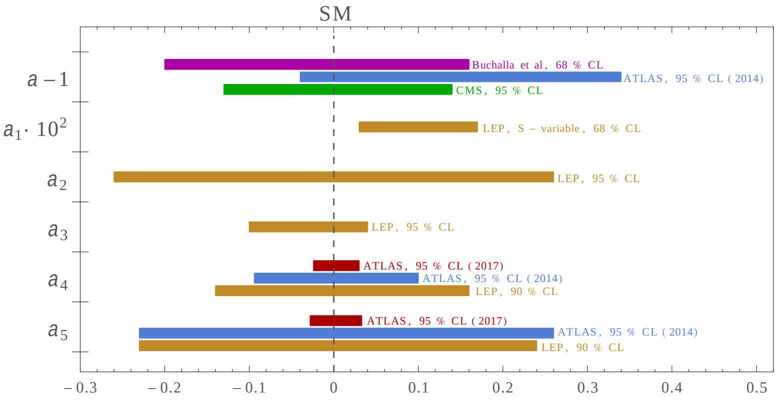

EW Chiral Lagrangian

$$
\begin{aligned}
\mathcal{L}_2 =& -\frac{1}{2g^2}\mathrm{Tr}\Big(\hat{W}_{\mu\nu}\hat{W}^{\mu\nu}\Big) - \frac{1}{2g'^2}\mathrm{Tr}\Big(\hat{B}_{\mu\nu}\hat{B}^{\mu\nu}\Big) \\
&+ \frac{v^2}{4}\left[1 + 2a\frac{H}{v} + b\frac{H^2}{v^2}\right]\mathrm{Tr}\Big(D^\mu U^\dagger D_\mu U\Big) + \frac{1}{2}\partial^\mu H\,\partial_\mu H + \dots\,, \\
\mathcal{L}_4 =&\ a_1\mathrm{Tr}\Big(U\hat{B}_{\mu\nu}U^\dagger\hat{W}^{\mu\nu}\Big) + ia_2\mathrm{Tr}\Big(U\hat{B}_{\mu\nu}U^\dagger[\mathcal{V}^\mu,\mathcal{V}^\nu]\Big) - ia_3\mathrm{Tr}\Big(\hat{W}_{\mu\nu}[\mathcal{V}^\mu,\mathcal{V}^\nu] \\
&+ a_4\Big[\mathrm{Tr}(\mathcal{V}_\mu\mathcal{V}_\nu)\Big]\Big[\mathrm{Tr}(\mathcal{V}^\mu\mathcal{V}^\nu)\Big] + a_5\Big[\mathrm{Tr}(\mathcal{V}_\mu\mathcal{V}^\mu)\Big]\Big[\mathrm{Tr}(\mathcal{V}_\nu\mathcal{V}^\nu)\Big] \\
&- c_W\frac{H}{v}\mathrm{Tr}\Big(\hat{W}_{\mu\nu}\hat{W}^{\mu\nu}\Big) - c_B\frac{H}{v}\mathrm{Tr}\Big(\hat{B}_{\mu\nu}\hat{B}^{\mu\nu}\Big) + \dots
\end{aligned}
$$

Proca Lagrangian

$$\mathcal{L}_V = -\frac{1}{4}\mathrm{Tr}(\hat{V}_{\mu\nu}\hat{V}^{\mu\nu}) + \frac{1}{2}M_V^2\mathrm{Tr}(\hat{V}_\mu\hat{V}^\mu)$$
$$+\frac{f_V}{2\sqrt{2}}\mathrm{Tr}(\hat{V}_{\mu\nu}f_+^{\mu\nu}) + \frac{ig_V}{2\sqrt{2}}\mathrm{Tr}(\hat{V}_{\mu\nu}[u^\mu, u^\nu])$$

Channels: $WZ \to WZ$

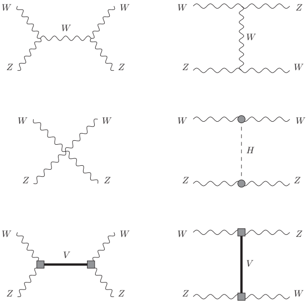

- Our Proca Lagrangian needs $g_v = g_v(z, s)$

$$g_V^2(z) = g_V^2(M_V^2)\frac{M_V^2}{z} \text{ for } s < M_V^2$$

$$g_V^2(z) = g_V^2(M_V^2)\frac{M_V^4}{z^2} \text{ for } s > M_V^2,$$

  $z = s,\ t,\ u$ depending on the channel where V propagates. Fully crossing symmetry leads to a moderate violation of the Froissart bound.

- We are using MadGraph v5 capability of integrating Fortran code inside UFO.
- We encode the Proca processes (those involving the resonace V) as effective vertices inside the UFO.
- The parameters of the Proca Lagrangian are adjusted to the IAM results [dynamic M_V, Γ_V, $g_V(M_V^2)$] via a custom piece of software.

Channels: $WZ \to WZ$

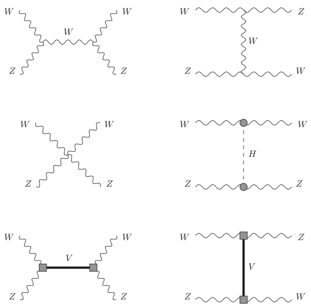

- Our Proca Lagrangian needs $g_v = g_v(z, s)$

$$g_V^2(z) = g_V^2(M_V^2)\frac{M_V^2}{z} \text{ for } s < M_V^2$$
$$g_V^2(z) = g_V^2(M_V^2)\frac{M_V^4}{z^2} \text{ for } s > M_V^2,$$

  $z = s,\ t,\ u$ depending on the channel where V propagates. Fully crossing symmetry leads to a moderate violation of the Froissart bound.

- We are using MadGraph v5 capability of integrating Fortran code inside UFO.

- We encode the Proca processes (those involving the resonace V) as effective vertices inside the UFO.

- The parameters of the Proca Lagrangian are adjusted to the IAM results [dynamic M_V, Γ_V, $g_V(M_V^2)$] via a custom piece of software.

Channels: $WZ \to WZ$

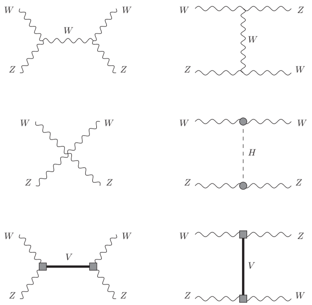

- Our Proca Lagrangian needs $g_v = g_v(z,s)$

$$g_V^2(z) = g_V^2(M_V^2)\frac{M_V^2}{z} \text{ for } s < M_V^2$$

$$g_V^2(z) = g_V^2(M_V^2)\frac{M_V^4}{z^2} \text{ for } s > M_V^2,$$

  $z = s,\ t,\ u$ depending on the channel where V propagates. Fully crossing symmetry leads to a moderate violation of the Froissart bound.

- We are using MadGraph v5 capability of integrating Fortran code inside UFO.
- We encode the Proca processes (those involving the resonace V) as effective vertices inside the UFO.
- The parameters of the Proca Lagrangian are adjusted to the IAM results [dynamic M_V, Γ_V, $g_V(M_V^2)$] via a custom piece of software.

Channels: $WZ \to WZ$

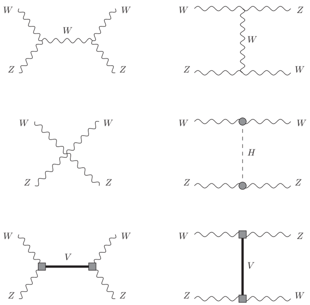

- Our Proca Lagrangian needs $g_v = g_v(z, s)$

$$g_V^2(z) = g_V^2(M_V^2)\frac{M_V^2}{z} \text{ for } s < M_V^2$$

$$g_V^2(z) = g_V^2(M_V^2)\frac{M_V^4}{z^2} \text{ for } s > M_V^2,$$

  $z = s,\ t,\ u$ depending on the channel where V propagates. Fully crossing symmetry leads to a moderate violation of the Froissart bound.

- We are using MadGraph v5 capability of integrating Fortran code inside UFO.
- We encode the Proca processes (those involving the resonance V) as effective vertices inside the UFO.

- The parameters of the Proca Lagrangian are adjusted to the IAM results [dynamic M_V, Γ_V, $g_V(M_V^2)$] via a custom piece of software.

Channels: $WZ \to WZ$

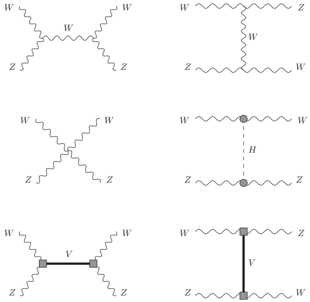

- Our Proca Lagrangian needs $g_v = g_v(z, s)$

$$g_V^2(z) = g_V^2(M_V^2)\frac{M_V^2}{z} \text{ for } s < M_V^2$$
$$g_V^2(z) = g_V^2(M_V^2)\frac{M_V^4}{z^2} \text{ for } s > M_V^2,$$

$z = s,\ t,\ u$ depending on the channel where V propagates. Fully crossing symmetry leads to a moderate violation of the Froissart bound.

- We are using MadGraph v5 capability of integrating Fortran code inside UFO.
- We encode the Proca processes (those involving the resonance V) as effective vertices inside the UFO.
- The parameters of the Proca Lagrangian are adjusted to the IAM results [dynamic M_V, Γ_V, $g_V(M_V^2)$] via a custom piece of software.

Channels: $WZ \to WZ$

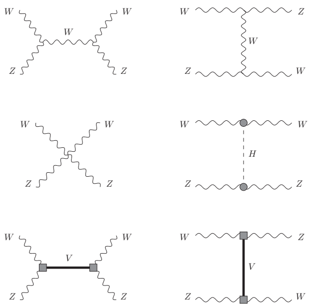

- Our Proca Lagrangian needs $g_v = g_v(z, s)$

$$g_V^2(z) = g_V^2(M_V^2)\frac{M_V^2}{z} \text{ for } s < M_V^2$$
$$g_V^2(z) = g_V^2(M_V^2)\frac{M_V^4}{z^2} \text{ for } s > M_V^2,$$

  $z = s,\ t,\ u$ depending on the channel where V propagates. Fully crossing symmetry leads to a moderate violation of the Froissart bound.

- We are using MadGraph v5 capability of integrating Fortran code inside UFO.
- We encode the Proca processes (those involving the resonance V) as effective vertices inside the UFO.

- The parameters of the Proca Lagrangian are adjusted to the IAM results [dynamic M_V, Γ_V, $g_V(M_V^2)$] via a custom piece of software.

Unitarization procedures for elastic processes

$$A^{IAM}(s) = \frac{[A^{(0)}(s)]^2}{A^{(0)}(s) - A^{(1)}(s)},$$

$$A^{N/D}(s) = \frac{A^{(0)}(s) + A_L(s)}{1 - \frac{A_R(s)}{A^{(0)}(s)} + \frac{1}{2}g(s)A_L(-s)},$$

$$A^{IK}(s) = \frac{A^{(0)}(s) + A_L(s)}{1 - \frac{A_R(s)}{A^{(0)}(s)} + g(s)A_L(s)},$$

$$A_0^K(s) = \frac{A_0(s)}{1 - iA_0(s)},$$

$$g(s) = \frac{1}{\pi}\left(\frac{B(\mu)}{D+E} + \log\frac{-s}{\mu^2}\right)$$

$$A_L(s) = \pi g(-s)Ds^2$$

$$A_R(s) = \pi g(s)Es^2$$

where

PRD **91** (2015) 075017

Unitarization procedures for elastic processes

$$A^{IAM}(s) = \frac{[A^{(0)}(s)]^2}{A^{(0)}(s) - A^{(1)}(s)},$$

$$A^{N/D}(s) = \frac{A^{(0)}(s) + A_L(s)}{1 - \frac{A_R(s)}{A^{(0)}(s)} + \frac{1}{2}g(s)A_L(-s)},$$

$$A^{IK}(s) = \frac{A^{(0)}(s) + A_L(s)}{1 - \frac{A_R(s)}{A^{(0)}(s)} + g(s)A_L(s)},$$

$$A_0^K(s) = \frac{A_0(s)}{1 - iA_0(s)},$$

where

$$g(s) = \frac{1}{\pi}\left(\frac{B(\mu)}{D+E} + \log\frac{-s}{\mu^2}\right)$$

$$A_L(s) = \pi g(-s) D s^2$$

$$A_R(s) = \pi g(s) E s^2$$

PRD **91** (2015) 075017

Unitarization procedures for elastic processes

$$A^{IAM}(s) = \frac{[A^{(0)}(s)]^2}{A^{(0)}(s) - A^{(1)}(s)},$$

$$A^{N/D}(s) = \frac{A^{(0)}(s) + A_L(s)}{1 - \frac{A_R(s)}{A^{(0)}(s)} + \frac{1}{2}g(s)A_L(-s)},$$

$$A^{IK}(s) = \frac{A^{(0)}(s) + A_L(s)}{1 - \frac{A_R(s)}{A^{(0)}(s)} + g(s)A_L(s)},$$

$$A_0^K(s) = \frac{A_0(s)}{1 - iA_0(s)},$$

where

$$g(s) = \frac{1}{\pi}\left(\frac{B(\mu)}{D+E} + \log\frac{-s}{\mu^2}\right)$$

$$A_L(s) = \pi g(-s) D s^2$$

$$A_R(s) = \pi g(s) E s^2$$

PRD **91** (2015) 075017

Unitarization procedures for elastic processes

$$A^{IAM}(s) = \frac{[A^{(0)}(s)]^2}{A^{(0)}(s) - A^{(1)}(s)},$$

$$A^{N/D}(s) = \frac{A^{(0)}(s) + A_L(s)}{1 - \frac{A_R(s)}{A^{(0)}(s)} + \frac{1}{2}g(s)A_L(-s)},$$

$$A^{IK}(s) = \frac{A^{(0)}(s) + A_L(s)}{1 - \frac{A_R(s)}{A^{(0)}(s)} + g(s)A_L(s)},$$

$$A_0^K(s) = \frac{A_0(s)}{1 - iA_0(s)},$$

where

$$g(s) = \frac{1}{\pi}\left(\frac{B(\mu)}{D+E} + \log\frac{-s}{\mu^2}\right)$$

$$A_L(s) = \pi g(-s) D s^2$$

$$A_R(s) = \pi g(s) E s^2$$

PRD **91** (2015) 075017

Matricial versions of the methods

$$F^{IAM}(s) = \left[F^{(0)}(s)\right]^{-1} \cdot \left[F^{(0)}(s) - F^{(1)}(s)\right] \cdot \left[F^{(0)}(s)\right]^{-1},$$

$$F^{N/D}(s) = \left[1 - F_R(s) \cdot \left(F^{(0)}(s)\right)^{-1} + \frac{1}{2} G(s) F_L(-s)\right]^{-1} \cdot N_0(s),$$

$$F^{IK}(s) = [1 + G(s) \cdot N_0(s)]^{-1} \cdot N_0(s),$$

where $G(s)$, $F_L(s)$, $F_R(s)$ and $N_0(s)$ are defined as

$$G(s) = \frac{1}{\pi}\left(B(\mu)(D+E)^{-1} + \log\frac{-s}{\mu^2}\right)$$

$$F_L(s) = \pi G(-s) D s^2$$

$$F_R(s) = \pi G(s) E s^2$$

$$N_0(s) = F^{(0)}(s) + F_L(s)$$

PRD **91** (2015) 075017

Matricial versions of the methods

$$F^{IAM}(s) = \left[F^{(0)}(s)\right]^{-1} \cdot \left[F^{(0)}(s) - F^{(1)}(s)\right] \cdot \left[F^{(0)}(s)\right]^{-1},$$

$$F^{N/D}(s) = \left[1 - F_R(s) \cdot \left(F^{(0)}(s)\right)^{-1} + \frac{1}{2} G(s) F_L(-s)\right]^{-1} \cdot N_0(s),$$

$$F^{IK}(s) = [1 + G(s) \cdot N_0(s)]^{-1} \cdot N_0(s),$$

where $G(s)$, $F_L(s)$, $F_R(s)$ and $N_0(s)$ are defined as

$$G(s) = \frac{1}{\pi}\left(B(\mu)(D+E)^{-1} + \log\frac{-s}{\mu^2}\right)$$

$$F_L(s) = \pi G(-s) D s^2$$

$$F_R(s) = \pi G(s) E s^2$$

$$N_0(s) = F^{(0)}(s) + F_L(s)$$

PRD **91** (2015) 075017

Matricial versions of the methods

$$F^{IAM}(s) = \left[F^{(0)}(s)\right]^{-1} \cdot \left[F^{(0)}(s) - F^{(1)}(s)\right] \cdot \left[F^{(0)}(s)\right]^{-1},$$

$$F^{N/D}(s) = \left[1 - F_R(s) \cdot \left(F^{(0)}(s)\right)^{-1} + \frac{1}{2}G(s)F_L(-s)\right]^{-1} \cdot N_0(s),$$

$$F^{IK}(s) = [1 + G(s) \cdot N_0(s)]^{-1} \cdot N_0(s),$$

where $G(s)$, $F_L(s)$, $F_R(s)$ and $N_0(s)$ are defined as

$$G(s) = \frac{1}{\pi}\left(B(\mu)(D+E)^{-1} + \log\frac{-s}{\mu^2}\right)$$

$$F_L(s) = \pi G(-s)Ds^2$$

$$F_R(s) = \pi G(s)Es^2$$

$$N_0(s) = F^{(0)}(s) + F_L(s)$$

PRD **91** (2015) 075017

Usability channel of unitarization procedures

IJ	00	02	11	20	22
Method of choice	Any	N/D IK	IAM	Any	N/D IK

- The IAM method cannot be used when $A^{(0)} = 0$, because it would give a vanishing value.
- The N/D and the IK methods cannot be used if $D + E = 0$, because in this case computing $A_L(s)$ and $A_R(s)$ is not possible.
- The naive K-matrix method,

$$A_0^K(s) = \frac{A_0(s)}{1 - iA_0(s)},$$

  fails because it is not analytical in the first Riemann sheet and, consequently, it is not a proper partial wave compatible with microcausality.

Usability channel of unitarization procedures

IJ	00	02	11	20	22
Method of choice	Any	N/D IK	IAM	Any	N/D IK

- The IAM method cannot be used when $A^{(0)} = 0$, because it would give a vanishing value.
- The N/D and the IK methods cannot be used if $D + E = 0$, because in this case computing $A_L(s)$ and $A_R(s)$ is not possible.
- The naive K-matrix method,

$$A_0^K(s) = \frac{A_0(s)}{1 - iA_0(s)},$$

fails because it is not analytical in the first Riemann sheet and, consequently, it is not a proper partial wave compatible with microcausality.

Usability channel of unitarization procedures

IJ	00	02	11	20	22
Method of choice	Any	N/D IK	IAM	Any	N/D IK

- The IAM method cannot be used when $A^{(0)} = 0$, because it would give a vanishing value.
- The N/D and the IK methods cannot be used if $D + E = 0$, because in this case computing $A_L(s)$ and $A_R(s)$ is not possible.
- The naive K-matrix method,

$$A_0^K(s) = \frac{A_0(s)}{1 - iA_0(s)},$$

fails because it is not analytical in the first Riemann sheet and, consequently, it is not a proper partial wave compatible with microcausality.

Unitarity problem

- VBS amplitude rises with energy, eventually leading to violation of unitarity at some new physics state.
- This leads to an *OVERESTIMATED* number of events in VBS due to an unphysical prediction of EFT. That is, amplitudes *cannot* grow uncontrolled.
- Exception, MSM: Higgs exchange exactly cancels this energy rise in VBS, restoring unitarity event at LO.
- Two options:
    - Set up a low-energy cut-off on the theory, due to the validity limits of the EFT itself. This limit, indeed, comes from the UV completion, whose specification would require to pick up a full (renormali. and unitar.) model from the *theory zoo*.
    - **Consider the EFT a valid low-energy limit and take advantage of the analytical properties of the scattering amplitudes, encoded in the so–called unitarization procedures, to extend the validity regime of the EFT. These techniques are well known from hadron physics.**

Unitarity problem

- VBS amplitude rises with energy, eventually leading to violation of unitarity at some new physics state.
- This leads to an *OVERESTIMATED* number of events in VBS due to an unphysical prediction of EFT. That is, amplitudes *cannot* grow uncontrolled.
- Exception, MSM: Higgs exchange exactly cancels this energy rise in VBS, restoring unitarity event at LO.
- Two options:
  - Set up a low-energy cut-off on the theory, due to the validity limits of the EFT itself. This limit, indeed, comes from the UV completion, whose specification would require to pick up a full (renormali. and unitar.) model from the *theory zoo*.
  - **Consider the EFT a valid low-energy limit and take advantage of the analytical properties of the scattering amplitudes, encoded in the so–called unitarization procedures, to extend the validity regime of the EFT. These techniques are well known from hadron physics.**

Unitarity problem

- VBS amplitude rises with energy, eventually leading to violation of unitarity at some new physics state.
- This leads to an *OVERESTIMATED* number of events in VBS due to an unphysical prediction of EFT. That is, amplitudes *cannot* grow uncontrolled.
- Exception, MSM: Higgs exchange exactly cancels this energy rise in VBS, restoring unitarity event at LO.
- Two options:
  - Set up a low-energy cut-off on the theory, due to the validity limits of the EFT itself. This limit, indeed, comes from the UV completion, whose specification would require to pick up a full (renormali. and unitar.) model from the *theory zoo*.
  - **Consider the EFT a valid low-energy limit and take advantage of the analytical properties of the scattering amplitudes, encoded in the so–called unitarization procedures, to extend the validity regime of the EFT. These techniques are well known from hadron physics.**

Unitarity problem

- VBS amplitude rises with energy, eventually leading to violation of unitarity at some new physics state.
- This leads to an *OVERESTIMATED* number of events in VBS due to an unphysical prediction of EFT. That is, amplitudes *cannot* grow uncontrolled.
- Exception, MSM: Higgs exchange exactly cancels this energy rise in VBS, restoring unitarity event at LO.
- Two options:
  - Set up a low-energy cut-off on the theory, due to the validity limits of the EFT itself. This limit, indeed, comes from the UV completion, whose specification would require to pick up a full (renormali. and unitar.) model from the *theory zoo*.
  - **Consider the EFT a valid low-energy limit and take advantage of the analytical properties of the scattering amplitudes, encoded in the so–called unitarization procedures, to extend the validity regime of the EFT. These techniques are well known from hadron physics.**

Unitarity problem

- VBS amplitude rises with energy, eventually leading to violation of unitarity at some new physics state.
- This leads to an *OVERESTIMATED* number of events in VBS due to an unphysical prediction of EFT. That is, amplitudes *cannot* grow uncontrolled.
- Exception, MSM: Higgs exchange exactly cancels this energy rise in VBS, restoring unitarity event at LO.
- Two options:
  - Set up a low-energy cut-off on the theory, due to the validity limits of the EFT itself. This limit, indeed, comes from the UV completion, whose specification would require to pick up a full (renormali. and unitar.) model from the *theory zoo*.
  - Consider the EFT a valid low-energy limit and take advantage of the analytical properties of the scattering amplitudes, encoded in the so–called unitarization procedures, to extend the validity regime of the EFT. These techniques are well known from hadron physics.

Unitarity problem

- VBS amplitude rises with energy, eventually leading to violation of unitarity at some new physics state.
- This leads to an *OVERESTIMATED* number of events in VBS due to an unphysical prediction of EFT. That is, amplitudes *cannot* grow uncontrolled.
- Exception, MSM: Higgs exchange exactly cancels this energy rise in VBS, restoring unitarity event at LO.
- Two options:
  - Set up a low-energy cut-off on the theory, due to the validity limits of the EFT itself. This limit, indeed, comes from the UV completion, whose specification would require to pick up a full (renormali. and unitar.) model from the *theory zoo*.
  - **Consider the EFT a valid low-energy limit and take advantage of the analytical properties of the scattering amplitudes, encoded in the so–called unitarization procedures, to extend the validity regime of the EFT. These techniques are well known from hadron physics.**

Unitarity problem: how bad is the problem?

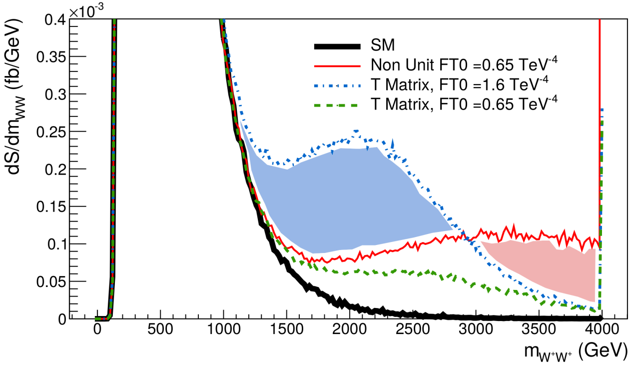

- T-matrix unit., [Sekulla et.al., *Particle Phenomen. Seminar*, 24/01/2017]
- f_{S_1}/Λ^4, $[-21.6, 21.8]$ (CMS, 13 TeV), $[-50.0, 60.3]$ (T-matrix)
- f_{M_0}/Λ^4, $[-8.7, 9.1]$ (CMS, 13 TeV), $[-1.35, 1.60]$ (T-matrix)
- f_{T_0}/Λ^4, $[-0.62, 0.65]$ (CMS, 13 TeV), $[-1.35, 1.60]$ (T-matrix)

Unitarity problem: how bad is the problem?

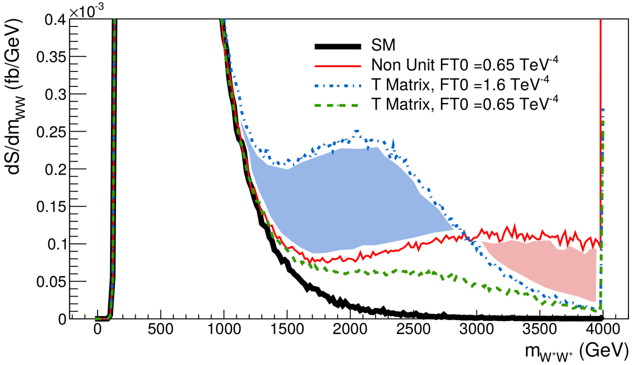

- T-matrix unit., [Sekulla et.al., *Particle Phenomen. Seminar*, 24/01/2017]
- f_{S_1}/Λ^4, $[-21.6, 21.8]$ (CMS, $13\,\mathrm{TeV}$), $[-50.0, 60.3]$ (T-matrix)
- f_{M_0}/Λ^4, $[-8.7, 9.1]$ (CMS, $13\,\mathrm{TeV}$), $[-1.35, 1.60]$ (T-matrix)
- f_{T_0}/Λ^4, $[-0.62, 0.65]$ (CMS, $13\,\mathrm{TeV}$), $[-1.35, 1.60]$ (T-matrix)

Unitarity problem: how bad is the problem?

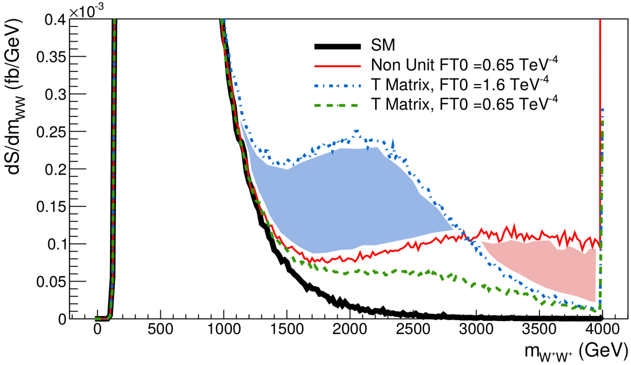

- T-matrix unit., [Sekulla et.al., *Particle Phenomen. Seminar*, 24/01/2017]
- f_{S_1}/Λ^4, $[-21.6, 21.8]$ (CMS, 13 TeV), $[-50.0, 60.3]$ (T-matrix)
- f_{M_0}/Λ^4, $[-8.7, 9.1]$ (CMS, 13 TeV), $[-1.35, 1.60]$ (T-matrix)
- f_{T_0}/Λ^4, $[-0.62, 0.65]$ (CMS, 13 TeV), $[-1.35, 1.60]$ (T-matrix)

Unitarity problem: how bad is the problem?

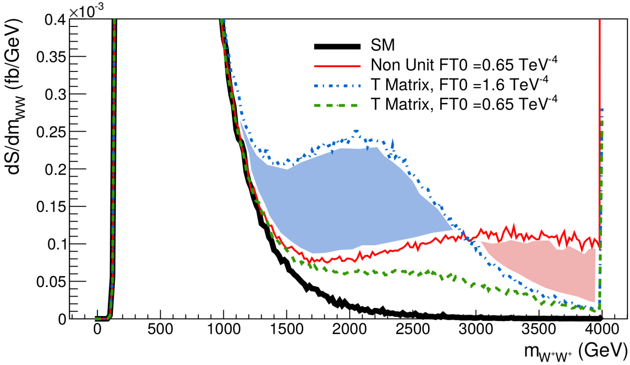

- T-matrix unit., [Sekulla et.al., *Particle Phenomen. Seminar*, 24/01/2017]
- f_{S_1}/Λ^4, $[-21.6, 21.8]$ (CMS, 13 TeV), $[-50.0, 60.3]$ (T-matrix)
- f_{M_0}/Λ^4, $[-8.7, 9.1]$ (CMS, 13 TeV), $[-1.35, 1.60]$ (T-matrix)
- f_{T_0}/Λ^4, $[-0.62, 0.65]$ (CMS, 13 TeV), $[-1.35, 1.60]$ (T-matrix)

Unitarity problem: unit. procedures

- *Zoo* of unitarization procedures: IAM, K-matrix, T-matrix, N/D, large-N,...
- They are applicable depending on the analytical properties of the EFT amplitude that is going to be unitarized.
- Depend on analytical continuation (Cauchy's theorem).

Unitarity problem: unit. procedures

- *Zoo* of unitarization procedures: IAM, K-matrix, T-matrix, N/D, large-N,...
- They are applicable depending on the analytical properties of the EFT amplitude that is going to be unitarized.
- Depend on analytical continuation (Cauchy's theorem).

Unitarity problem: unit. procedures

- *Zoo* of unitarization procedures: IAM, K-matrix, T-matrix, N/D, large-N,...
- They are applicable depending on the analytical properties of the EFT amplitude that is going to be unitarized.
- Depend on analytical continuation (Cauchy's theorem).

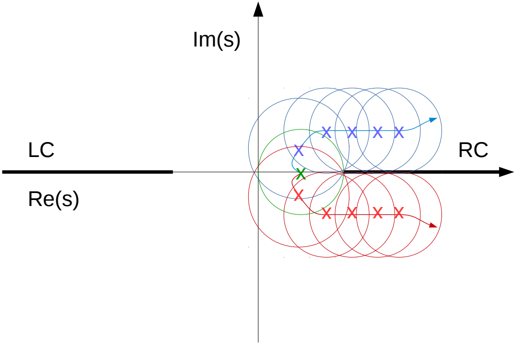

Unitarity problem: other view of unit. procedures

- However, in collider phenomenology we are used to a very similar situation:
- RESUMMATION

Unitarity problem: other view of unit. procedures

- However, in collider phenomenology we are used to a very similar situation:
- RESUMMATION

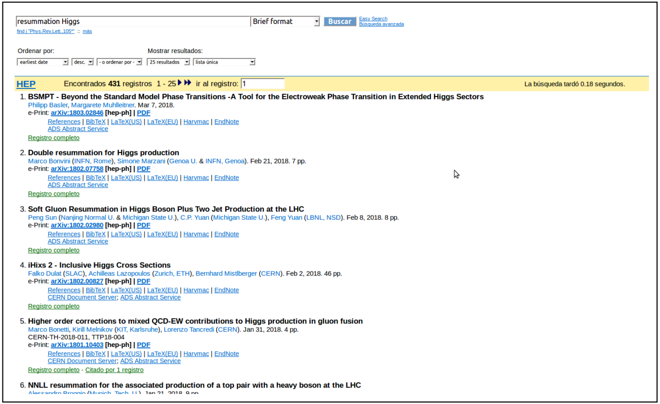

resummation Higgs | Brief format | Buscar | Easy Search | Búsqueda avanzada

find j "Phys.Rev.Lett.,105*" :: más

Ordenar por: earliest date | desc. | - o ordenar por -

Mostrar resultados: 25 resultados | lista única

HEP Encontrados **431** registros 1 - 25 ▶ ⏩ ir al registro: 1 La búsqueda tardó 0.18 segundos.

1. **BSMPT - Beyond the Standard Model Phase Transitions -A Tool for the Electroweak Phase Transition in Extended Higgs Sectors**
   Philipp Basler, Margarete Muhlleitner. Mar 7, 2018.
   e-Print: **arXiv:1803.02846 [hep-ph] | PDF**
   References | BibTeX | LaTeX(US) | LaTeX(EU) | Harvmac | EndNote
   ADS Abstract Service
   Registro completo
2. **Double resummation for Higgs production**
   Marco Bonvini (INFN, Rome), Simone Marzani (Genoa U. & INFN, Genoa). Feb 21, 2018. 7 pp.
   e-Print: **arXiv:1802.07758 [hep-ph] | PDF**
   References | BibTeX | LaTeX(US) | LaTeX(EU) | Harvmac | EndNote
   ADS Abstract Service
   Registro completo
3. **Soft Gluon Resummation in Higgs Boson Plus Two Jet Production at the LHC**
   Peng Sun (Nanjing Normal U. & Michigan State U.), C.P. Yuan (Michigan State U.), Feng Yuan (LBNL, NSD). Feb 8, 2018. 8 pp.
   e-Print: **arXiv:1802.02980 [hep-ph] | PDF**
   References | BibTeX | LaTeX(US) | LaTeX(EU) | Harvmac | EndNote
   ADS Abstract Service
   Registro completo
4. **iHixs 2 - Inclusive Higgs Cross Sections**
   Falko Dulat (SLAC), Achilleas Lazopoulos (Zurich, ETH), Bernhard Mistlberger (CERN). Feb 2, 2018. 46 pp.
   e-Print: **arXiv:1802.00827 [hep-ph] | PDF**
   References | BibTeX | LaTeX(US) | LaTeX(EU) | Harvmac | EndNote
   CERN Document Server; ADS Abstract Service
   Registro completo
5. **Higher order corrections to mixed QCD-EW contributions to Higgs production in gluon fusion**
   Marco Bonetti, Kirill Melnikov (KIT, Karlsruhe), Lorenzo Tancredi (CERN). Jan 31, 2018. 4 pp.
   CERN-TH-2018-011, TTP18-004
   e-Print: **arXiv:1801.10403 [hep-ph] | PDF**
   References | BibTeX | LaTeX(US) | LaTeX(EU) | Harvmac | EndNote
   CERN Document Server; ADS Abstract Service
   Registro completo - Citado por 1 registro
6. **NNLL resummation for the associated production of a top pair with a heavy boson at the LHC**
   Alessandro Broggio (Munich, Tech. U.). Jan 21, 2018. 9 pp.

Unitarity problem: other view of unit. procedures

- However, in collider phenomenology we are used to a very similar situation:
- RESUMMATION

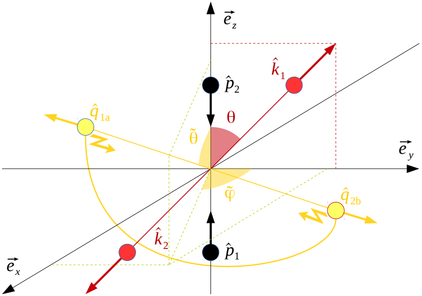

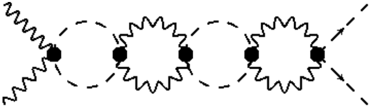

Typical Feynman diagram mixing the $\omega\omega$ and the *hh* channels. [PRL**114**, 221803]

WW hadronic final state, PRELIMINAR: BP1, W^+W^- in final state

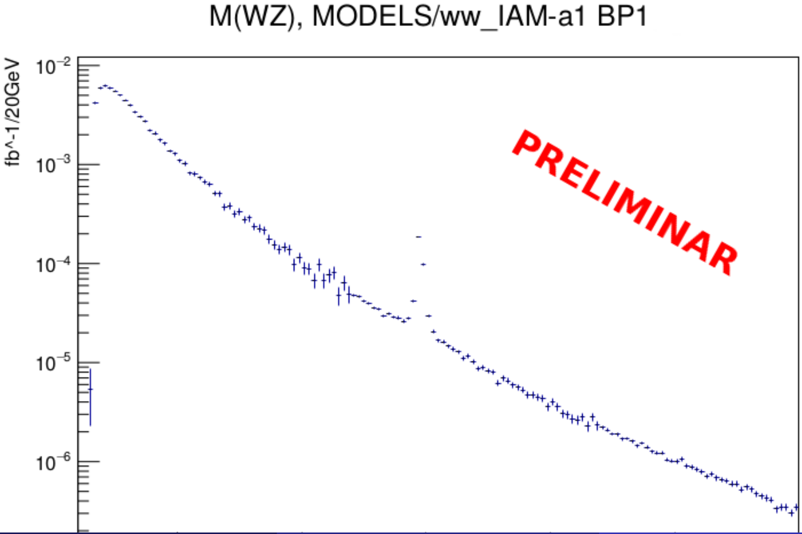

WW hadronic final state, PRELIMINAR: all BPs vs. background

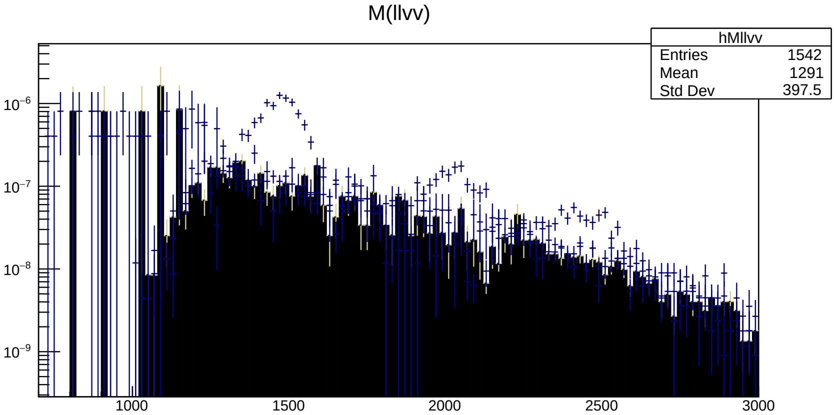

Reconstructed signal of BP1, BP2, BP3 (blue). EW backgr. (black)

WW hadronic final state, PRELIMINAR: $t\bar{t}$ background

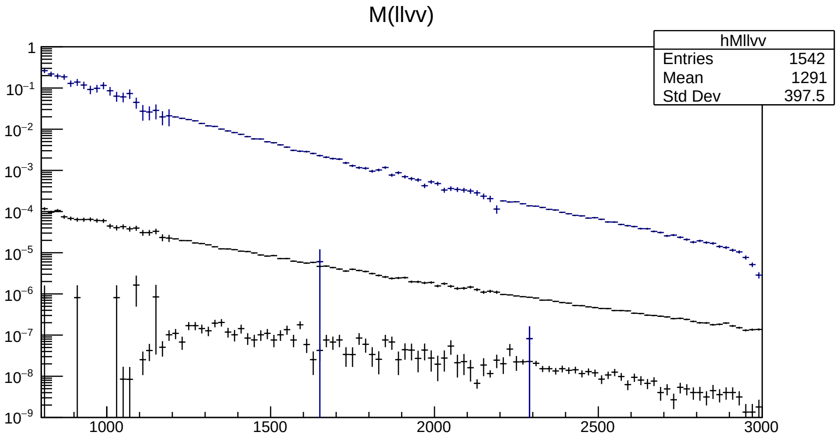

Blue: $pp \to t\bar{t} \to b\bar{b}W^+W^-$ background. Black: irred. EW background.

Upper curves: before Pythia8+Delphes cuts. I.e., only VBF cuts. NO b-tagging.